Structural Context of Mid-Tertiary Mineralization in the Mammoth and San Manuel Districts, Southeastern Arizona

U.S. GEOLOGICAL SURVEY BULLETIN 2042-C

Chapter C

Structural Context of Mid-Tertiary Mineralization in the Mammoth and San Manuel Districts, Southeastern Arizona

By ERIC R. FORCE and LESLIE J. COX

Three generations of extensional faulting and associated tilting affected mid-Tertiary mineralization of the Mammoth vein set and the newly described Shultz Spring altered area

U.S. GEOLOGICAL SURVEY BULLETIN 2042-C

MINERAL RESOURCE STUDIES ALONG THE
SIERRITA-MOGOLLON TRANSECT, ARIZONA-NEW MEXICO

U.S. DEPARTMENT OF THE INTERIOR
MANUEL LUJAN, JR., Secretary

U.S. GEOLOGICAL SURVEY
Dallas L. Peck, Director

UNITED STATES GOVERNMENT PRINTING OFFICE, WASHINGTON : 1992

For sale by
Book and Open-File Report Sales
U.S. Geological Survey
Federal Center, Box 25286
Denver, CO 80225

Library of Congress Cataloging in Publication Data

Force, Eric R.
Structural context of mid-Tertiary mineralization in the Mammoth and San Manuel districts, southeastern Arizona : three generations of extensional faulting and associated tilting affected mid-Tertiary mineralization of the Mammoth vein set and the newly described Shultz Spring altered area / by Eric R. Force and Leslie J. Cox.
p. cm.—(Mineral resource studies along the Sierrita-Mogollon Transect, Arizona-New Mexico ; ch. C) (U.S. Geological Survey bulletin ; 2042)
Includes bibliographical references.
1. Geology, Structural—Arizona. 2. Geology, Stratigraphic—Tertiary. 3. Metallogeny—Arizona. I. Cox, Leslie J. II. Title. III. Series. IV. Series: U.S. Geological Survey bulletin ; 2042.
QE75.B9 no. 2042
[QE627.5.A6]
557.3 s—dc20
[549.9791]

92-30105
CIP

CONTENTS

PLATE

FIGURES

TABLES

Structural Context of Mid-Tertiary Mineralization in the Mammoth and San Manuel Districts, Southeastern Arizona

By Eric R. Force *and* Leslie J. Cox

Abstract

The Mammoth district of Au, Ag, Mo, V, Pb, Zn vein deposits of mid-Tertiary age (22.0 to 22.5 Ma) spatially overlaps the San Manuel porphyry copper district of late Cretaceous to early Tertiary age, and shares its mid-Tertiary extensional history. Host rocks of the Mammoth vein set include rocks as young as the upper Oligocene to lower Miocene Cloudburst Formation, a thick syn-extensional pile of intermediate volcanic rocks and conglomerate, and associated rhyolite of extrusive and very shallow intrusive origin. The Mammoth vein set itself is emplaced into a fault, subsequently rotated, that originated as a high-angle oblique reverse fault with about 35 m (115 ft) of dip-slip movement and an unknown amount of right-lateral movement.

The Shultz Spring altered area to the southwest, described here for the first time, is also hosted by the Cloudburst Formation. It shows concentric alteration zones of pyrite and hematite-chlorite and weak Ba, Ag, Pb, Mo, Au, Cu mineralization. No continuous vein set is present.

Three episodes of extensional faulting have influenced the configuration of mid-Tertiary mineralization. These are described from youngest to oldest:

1. Basin-range faulting on the steeply northeast-dipping Mammoth fault zone has cut the steeply southwest-dipping vein into the Collins and Mammoth-Tiger segments, by down-to-the-northeast dip-slip movement of 264±2 m (866± 6 ft), calculated from the intersections of three planar features with the fault plane. The two segments when reconstructed represent 550 m (1,800 ft) of vertical relief to the lowest exploited level.

2. Low-angle normal faulting on two splays of the southwest-dipping San Manuel fault system, concurrent with accumulation of the lower Miocene San Manuel Formation, and with northeast tilting of about 25°, clearly postdates the Mammoth vein set. However, these veins have not been found on the upper plate of the faults. Recalculation of total offset on the San Manuel fault system yields approximately 2,363 m (7,750 ft) of separation, top toward S. 46° W. This vector prohibits the Shultz Spring altered area from being a correlative feature; instead the Ford mine area on the lower plate of the fault system may correlate with the Shultz Spring area, and the Mammoth vein set probably has been eroded from the upper plate.

3. The Cloudburst detachment fault, now horizontal, formed concurrently with the Cloudburst Formation and rotated it about 30° to the northeast. The Turtle fault apparently bounds both the detachment and this rotation on the south and functioned as a side ramp for detachment. The Mammoth vein set cuts the Turtle fault, but close spatial and temporal relation of the vein set with the detachment suggests a genetic relation also: (1) The vein itself and concentric zones of mineral assemblages within it are centered under the intersection of the detachment surface with its side ramp, and (2) the vein set is coextensive with intrusive rhyolite, and apparently formed as rhyolite cooled. Rhyolite intrusion is demonstrably coeval with detachment. Detachment must have affected mineralization in some way; probably the oxide-dominated mineral assemblages are such an effect.

Extensive epidote-chlorite alteration extends above the Cloudburst fault plane about 60 m (200 ft) into the Cloudburst Formation. Those segments of the Mammoth vein set emplaced in the Cloudburst Formation show further wallrock epidotization, with the same alteration roof, again suggesting close temporal relations of detachment and veining. Structural extrapolation from nearby detachment outcrops suggests that below elevations of about 2,900 ft (885 m), the vein set is entirely in the lower plate of the Cloudburst detachment system.

Other conclusions reached in this paper are (1) the northeast splay of the San Manuel fault system moved most recently, based on stratigraphic relations in the San Manuel Formation, (2) the unconformity between the Oracle Granite and the Cloudburst Formation forms a structural marker in wallrocks of the Mammoth vein set but is camouflaged by rhyolite intrusion, and (3) the Laramide porphyry copper deposit at the San Manuel mine was probably tilted only about 25° to 30° by mid-Tertiary extension.

INTRODUCTION

The San Manuel and Mammoth mining districts are spatially overlapping centers of mineralization of late

Manuscript approved for publication, July 14, 1992.

Cretaceous to early Tertiary (henceforth Laramide) and mid-Tertiary age, respectively, on the flanks of the Black Hills, facing the San Pedro valley of southeastern Arizona (fig. 1). San Manuel is a large porphyry copper deposit, mined since 1946, well described by Schwartz (1953), Pelletier and Creasey (1965), and Thomas (1966). The Mammoth district, described by Peterson (1938) and Creasey (1950), is a vein set that has produced gold, silver, vanadium, molybdenum, lead, zinc, minor copper, and silica (for flux) at various times since first exploited in 1879. The San Manuel deposit has been the subject of a classic analysis of alteration geometry and post-mineral low-angle normal faulting (Lowell, 1968; Lowell and Guilbert, 1970), which led to discovery of the offset Kalamazoo segment of the orebody in subsurface. This study examines mid-Tertiary mineralization of the area in the context of both detachment and basin-range faulting. The surface geochemistry of a previously undescribed area of alteration is included. Force is responsible for geology and Cox is responsible for geochemistry.

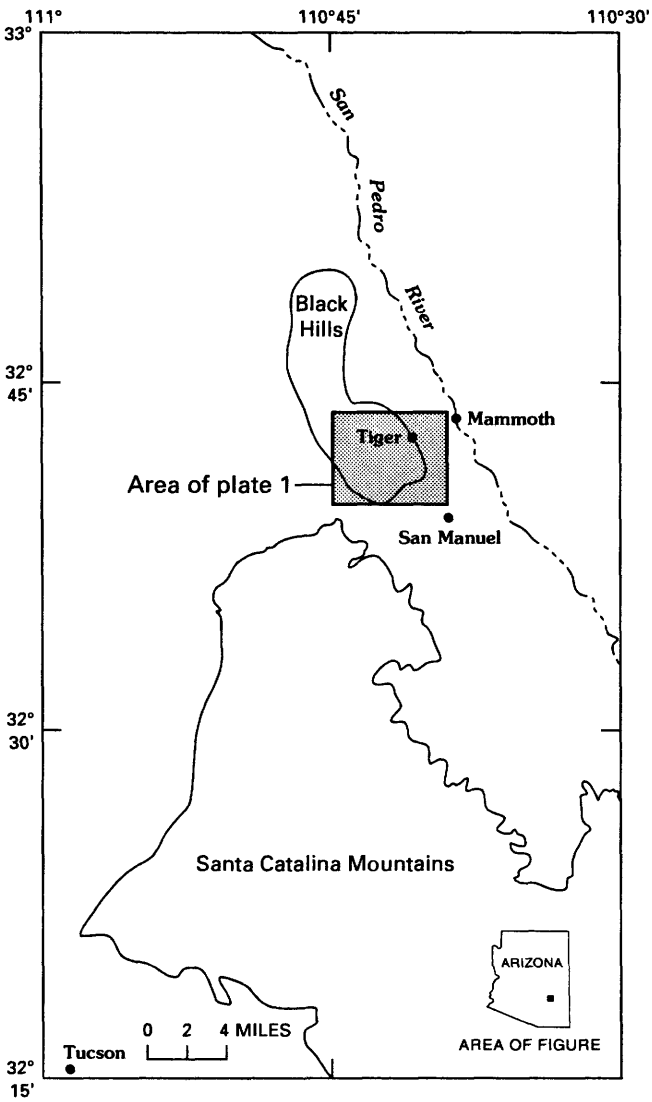

Figure 1. Index map of study area in southeastern Arizona showing area of plate 1 and town names. San Pedro River runs through San Pedro basin.

PRESENT STATUS OF GEOLOGIC KNOWLEDGE

Geology of the study area is quite complex, and our knowledge of it is changing rapidly. Included in this section are some previously unpublished observations.

Geologic Units

Igneous rocks of the map area (pl. 1) are of Middle Proterozoic, Laramide (Late Cretaceous to early Tertiary), and mid-Tertiary ages. Sedimentary rocks older than mid-Tertiary are absent.

Precambrian Granitic Rocks

The oldest rocks in the Mammoth district are granitic, the most important being the Oracle Granite (Yg on pl. 1) of Peterson (1938), about 1.4 Ga. The Oracle is extensively cut by aplite and lesser pegmatite (Yap), and by younger diabase (Ydb; about 1.1 Ga). The Oracle is locally altered and (or) mineralized near the San Manuel (and Kalamazoo) deposits (Lowell and Guilbert, 1970), but is not deformed. It is coarse grained and has large perthitic phenocrysts of potassium feldspar.

Granitic Porphyry of San Manuel Mine

Intrusive into the Oracle Granite is gray porphyry with prominent white plagioclase phenocrysts, commonly called San Manuel porphyry (henceforth this term is used). Two phases are present (see Thomas, 1966, for differences), but are not divided on this map (pl. 1). Both are presumably Laramide in age. Compositions are variously reported as granodioritic (Creasey, 1965), monzonitic (Schwartz, 1953), and quartz monzonitic (Thomas, 1966). The porphyry is variably altered and mineralized; the San Manuel copper deposit is centered on the porphyry (Lowell, 1968), and the porphyry and the Oracle Granite are its host rocks.

Cloudburst Formation

Heindl (1963) introduced the term Cloudburst Formation for conglomerate and volcanic rocks forming a thick section tilted to the northeast in the study area. The formation has since proved to be of late Oligocene and early Miocene age (Dickinson and Shafiqullah, 1989); that is,

contemporaneous with extension related to widespread detachment faulting in southeastern Arizona. Discordant intrusives (Ti) of the same general age are present in the map area, also.

The Cloudburst Formation is subdivided into a lower member (Tcl) that consists of volcanic rocks with lesser conglomerate, and an upper member (Tcu) that consists of conglomerate with minor pyroclastics and one thin flow (Weibel, 1981). The thickness of the lower member is estimated as 1,500 to 2,450 m (5,000 to 8,000 ft) from a base outside the area of plate 1, and that of the upper member, bounded above by an unconformity, is estimated as 2,130 m (7,000 ft). Volcanic rocks of the lower member are mostly of intermediate composition, some fragmental. Conglomerate in the lower member has mixed sources; clasts of Oracle Granite and rocks related to it in a provenance sense (Precambrian diabase and aplite; porphyry, some clasts altered and (or) mineralized) may be either less or more abundant than angular volcanic fragments. Some of the volcanic conglomerate beds probably represent lahars.

Near the Mammoth district, rhyolite of both intrusive and extrusive origin, including ash-flow tuff, is present toward the top of the lower member. Similar rhyolite north of the study area has been dated at 23 Ma (Dickinson and Shafiqullah, 1989).

The upper member of the Cloudburst Formation, consisting almost entirely of conglomerate, itself contains a lower zone characterized by volcanic clasts and an upper zone characterized by clasts of Oracle Granite and related rocks (Weibel, 1981). The boundary (pl. 1) coincides approximately with an arenite unit (Tcua). A volcanic flow (Tcuv) is in the lower zone. Sedimentary transport was toward the east throughout, according to Weibel; this is evaluated below. All of the conglomerate has an iron-rich matrix that is most commonly red-orange to purple-gray but in alteration zones described below the matrix is green or rusty.

Weibel (1981) traced a light-colored compound tuff-breccia (Tcut) near the top of the upper member for over 2 km (pl. 1) and dated potassium feldspar from it at 22.5 Ma. The significance of this date is discussed below.

San Manuel Formation

Heindl (1963) introduced the San Manuel Formation for conglomerate that is less tilted, less indurated, unaltered, and paler in matrix color than conglomerate of the underlying Cloudburst Formation. The contact between the Cloudburst and the overlying San Manuel appears to be conformable (and gradational in matrix color) in one area, and the contact is difficult to map in such sections. However, an unconformity is apparent (pl. 1) where the San Manuel Formation overlaps the tuff of the upper Cloudburst Formation. The absence of intrusions or of any alteration (of either hydrothermal or contact-metamorphic type) in the San Manuel, and the incorporation in it of clasts of rhyolite and altered Cloudburst, also suggest some regional significance of the unconformity separating the two formations. Very little time is represented by this unconformity, as basal San Manuel Formation gives ages of 22 Ma (Dickinson and Shafiqullah, 1989). Heindl (1963) recognized two members of the San Manuel Formation, the underlying Kannally Member (Tsml), defined by a predominance of Oracle Granite and related detritus, and the overlying Tucson Wash Member (Tsmu), defined by clasts of Cloudburst Formation (conglomerate and volcanic rocks). The contact between members corresponds to a change from easterly to southwesterly sediment transport (Dickinson, 1991). We find that the Tucson Wash Member is further divisible into two parts (not mapped). The lower part (the only part exposed in Tucson Wash itself) is characterized by clasts of the Cloudburst Formation (mostly volcanogenic conglomerate, some with secondary epidote), of rhyolite, of Mammoth vein quartz, and in the portion south of San Manuel mine, of mineralized porphyry. These clasts must have come from the northeast (pl. 1). The upper part consists of volcanic detritus and is best exposed in the open pit of the San Manuel mine. The lower part of the Tucson Wash Member rests directly on the Cloudburst Formation in one area, discussed below.

Quiburis Formation

Basin fill of the San Pedro valley to the east is called the Quiburis Formation (Tq; Heindl, 1963). Within the map area it consists of gravel dipping northeast about 5°; locally the dip is steep against the Mammoth, Cholla, and related faults that bound the formation on the west. The Quiburis Formation is post-mid-Miocene in age (Dickinson and Shafiqullah, 1989).

Major Faults

The map area contains so many faults of different ages that reconstruction is an intricate puzzle. The faults are described in apparent order of age from oldest to youngest.

Cloudburst and Turtle Faults

The subhorizontal Cloudburst fault (of Dickinson, 1987) forms a structural floor for exposed units north of the Turtle fault. Where the Cloudburst fault is exposed in the northwestern part of the map area (pl. 1), it dips gently eastward and separates Precambrian granitic rocks from overlying Cloudburst Formation that dips steeply northeast. The Cloudburst fault is thus a detachment fault and is thought to be of regional importance in the San Pedro-Santa Catalina Mountains area (Dickinson, 1991).

The Turtle fault separates the Oracle Granite and related rocks on the southeast from the Cloudburst Formation to the northwest. The fault is delineated by earlier work only in the San Manuel-Mammoth area, but Dickinson (1987) showed that a corresponding fault is present to the southwest on the upper plate of the younger San Manuel fault. Both segments of the Turtle fault dip 50° or more northwestward, with apparent movement being up-to-the-southeast.

Two lines of evidence suggest that the Turtle fault was active during deposition of the Cloudburst Formation: (1) The lower portions of the Cloudburst Formation are truncated against the fault, but upper portions overlap the fault (on both plates of the younger San Manuel fault) and rest unconformably on the Oracle Granite (fig. 2; pl. 1), and (2) the fault plane of the Turtle fault has been altered as much as the adjacent Cloudburst Formation and is cut by every post-depositional fault that cuts the Cloudburst Formation. Thus the Turtle fault must be about the same age as the Cloudburst Formation. Dickinson (1991) suggests that the Turtle fault is a tear or ramp fault related to the Cloudburst detachment system, which is known to have controlled Cloudburst deposition.

A late stage of movement on the Turtle fault was apparently down-to-the-south (pl. 1; fig. 2). The resulting minor offsets are the basis on which Peterson (1938) and Creasey (1965) mapped the Turtle fault into the Cloudburst Formation east of the Mammoth fault.

San Manuel Fault System

The map pattern of plate 1 reflects the San Manuel fault system more clearly than any other single structure. The fault juxtaposes older rocks to the northeast against younger rocks to the southwest and dips gently southwest. In the San Manuel mine, for example, the Oracle Granite is structurally overlain by the San Manuel Formation dipping northeastward into a fault plane that dips southwest. The San Manuel fault system has been interpreted as a thrust fault, a strike-slip fault, and a normal fault by various investigators. Lowell (1968) proved it to be a low-angle normal fault by correlating alteration, mineralization, and intrusive features between the San Manuel porphyry copper deposit and its structurally overlying Kalamazoo segment in the subsurface to the southwest. In so doing he verified suggestions of fault movement first made by Steele and Rubly (1947). Lowell's landmark paper, and a subsequent one by Lowell and Guilbert (1970), became models of both porphyry alteration geometry and detachment faulting. The fault separation listed by Lowell has the upper block translated about 2,440 m (8,000 ft) along an average dip of 25° to 30°, toward S. 55° W. We independently derive a slightly different vector in this paper.

Creasey (1965) recognized that two en echelon segments of the San Manuel fault are present in one area. Our map (pl. 1) extends the area between the two segments of the fault.

Dickinson (1991) presents evidence that the San Manuel Formation was deposited synchronously with and in response to movement on the San Manuel fault. In addition, we find that the lower part of the Tucson Wash Member, rather than the Kannally Member, is the basal lithology of the formation everywhere northeast of the southwest splay of the fault. Blocks of rhyolite and epidotic Cloudburst Formation, some large enough to be mapped by Creasey (1965), are incorporated in the basal Tucson Wash Member against the northeast splay of the fault, suggesting that this splay was active during deposition. This in turn suggests that the northeastern splay of the fault moved more recently, since the Tucson Wash is the upper member toward the southeast where the section is more complete. Derivation of the blocks was apparently from north of the Turtle fault, consistent with its down-to-the-south late movement.

Mammoth and Cholla Faults

Along the eastern side of the map area, steep east-dipping basin-and-range faults have dropped the San Pedro basin down relative to the Black Hills. Most prominent among these in the map area are the Mammoth and Cholla faults, which locally drop Quiburis Formation to the east against Oracle Granite to the west. These faults also cut and offset the Turtle fault and the San Manuel fault.

Terminology of these faults is confused. Early workers refer to a Mammoth fault, tentatively correlated with the East fault of the San Manuel mine, and to a Cholla fault east of it. The two converge to the northwest in the Tiger-Mammoth area. Creasey (1965) in both map and text refers to the Cholla fault of earlier workers as the Mammoth fault, but Pelletier and Creasey (1965) in the same report use the original terminology. Our map uses the Cholla fault in the original sense, as have other post-1965 workers (Thomas, 1966). Subsurface information shows that east-side downthrow on the Cholla fault decreases northwestward from about 210 to 90 m (700 to 300 ft) near Tiger (Schwartz, 1953). The Cholla fault is intimately related to the older Dream vein (not mapped separately) as discussed below. In the Mammoth-Tiger area and northward, one can consider fault movement as occurring on a single Mammoth fault zone.

The Mammoth Vein Set--General Description and Past Work

Veins of the Mammoth set were mined discontinuously from 1879 to 1959, with about 2 million tons of ore removed. Effort was primarily directed at gold in the early years of production; the total recovery was about 400,000 ounces (Creasey, 1950). In later years, silver (about 1 mil-

lion ounces), molybdenum (over 6 million pounds MoO_3), vanadium (over 2.5 million pounds V_2O_5), lead (over 70 million pounds), zinc (about 50 million pounds), and minor copper were the main products. In 1978, Magma Copper Company began mining the veins for silica, and recovered gold and silver. Total production listed by Keith and others (1983) is listed in table 1.

Geometry and grade of the veins are not well described. Individual veins may be as wide as 2 m (6 ft), but are most commonly a few centimeters wide, confined to zones locally over 10 m (33 ft) in width. Grades of gold were in the range 1 to 15 parts per million. In sulfide-rich zones, lead and zinc could each be over 5 percent (Creasey, 1950). Production figures in Creasey's table 5 imply that MoO_3 and V_2O_5 grades were about 2,500 and 1,000 ppm, respectively, in some segments of the veins.

The veins are emplaced along old faults (called vein-faults in Peterson, 1938) and consist largely of multiple stages of both quartz and entrained fault gouge. Early veins also contain adularia and later veins, calcite. Gold values were highest in finely banded quartz of intermediate age. Specularite-rich zones are characteristic, as are open-space-filling amethyst, wulfenite, and vanadinite. Manganese oxide, barite, and fluorite are common both in the veins and in joints in wallrock. A detailed paragenesis of minerals is given by Peterson (1938) and Creasey (1950).

The veins are approximately co-extensive with a zone of rhyolite intrusive and extrusive rocks that extends northwestward from Tiger across Tucson Wash (pl. 1). Some of the higher gold values were obtained where the veins cut these rhyolite bodies.

The Mammoth vein set now consists of two main segments, the Collins and the Mammoth-Tiger segments, on opposite walls of the Mammoth fault zone (fig. 2). The veins dip steeply, mainly southwest, whereas the Mammoth fault dips steeply northeast. The Mammoth-Tiger vein segment to the east has apparently dropped down relative to the Collins vein segment to the west. The amount of separation has been listed as about 210 m (700 ft) by Creasey (1950). This will be discussed in a following section.

In both these segments, mining of the veins was mostly south of the Turtle fault, where the Oracle Granite and the Cloudburst Formation are the main host rocks. The Collins segment was traced with little offset across the Turtle fault (fig. 2) and northwestward for over a kilometer by Creasey (1965).

Peterson (1938) and Creasey (1950) differed on the part played by supergene oxidation in the mineral assemblage of the veins, particularly wulfenite and vanadinite. Peterson regarded these minerals to be original though somewhat late-stage hydrothermal minerals whose concentration maxima represent a depth zone in the originally continuous vein, whereas Creasey believed the minerals are a result of weathering, partly before and partly after offset on the Mammoth fault. Creasey thus considered maxima of wulfenite and vanadinite to be a function of weathering depth and duration of exposure (the Collins vein segment having been exposed only after offset on the Mammoth fault).

Table 1. Production figures listed by Keith and others (1983) for the Mammoth district, Arizona, for the period 1886 to 1981

[--, no data]

Commodity	Quantity[1]		Apparent grade[2]
Ore	5,310,000	st	--
Au	349,000	oz	0.07 oz/ton
Ag	1,660,000	oz	0.31 oz/ton
Mo	3,943,046	lb	--
V	2,540,842	lb	--
Pb	132,680,000	lb	12.5 percent
Zn	87,312,000	lb	8.2 percent
Cu	10,445,000	lb	0.98 percent
Mn	41,600	lb	--
U	0		--

[1] st, short tons; oz, ounces; lb, pounds.
[2] Assumes recovery of all commodities.

Sequence of Events

The geologic features discussed thus far seem to fit the following post-Laramide sequence of events:

1. Accumulation of the Cloudburst Formation volcanic rocks and conglomerates, synchronous with and in response to movement on the Cloudburst and Turtle faults. Intrusion of intermediate to rhyolitic rocks accompanied sedimentation and faulting, as did the first stages of tilting to the northeast. Formation of the vein-faults and the Mammoth vein set was a late stage of this same generation of events.

2. Accumulation of the San Manuel Formation, in response to movement on the San Manuel fault, southwest segment first, accompanied by further tilting to the northeast and slight reversal of movement on the Turtle fault.

3. Uplift of the Black Hills relative to the San Pedro basin by down-to-the-east basin-and-range faulting on the Mammoth, Cholla, and related faults; accumulation of Quiburis Formation and final slight tilting to the northeast.

NEW WORK ON THE MAMMOTH VEIN SET

Our work with the Mammoth vein set is directed toward using regional geologic relations to constrain the structural evolution of the mineral deposits. The Collins segment of the vein set is discussed first, as it is less disturbed by later

faults (pl. 1, section *B-B'*). The relation of these faults in three dimensions is shown schematically in figure 3.

The Collins Vein Segment

The Collins vein segment is that to the west of the Mammoth fault zone, on the lower plate of the San Manuel fault system; that is, it is part of the same crustal block as the San Manuel porphyry copper deposit. The Collins vein segment trends northwest from its surface intersection with the Mammoth fault (fig. 2), across the hill (3,400 ft or 1,035 m elevation) in which the Collins workings were developed. From there it is poorly exposed downslope to Tucson Wash (2,870 ft or 865 m), across the Turtle fault

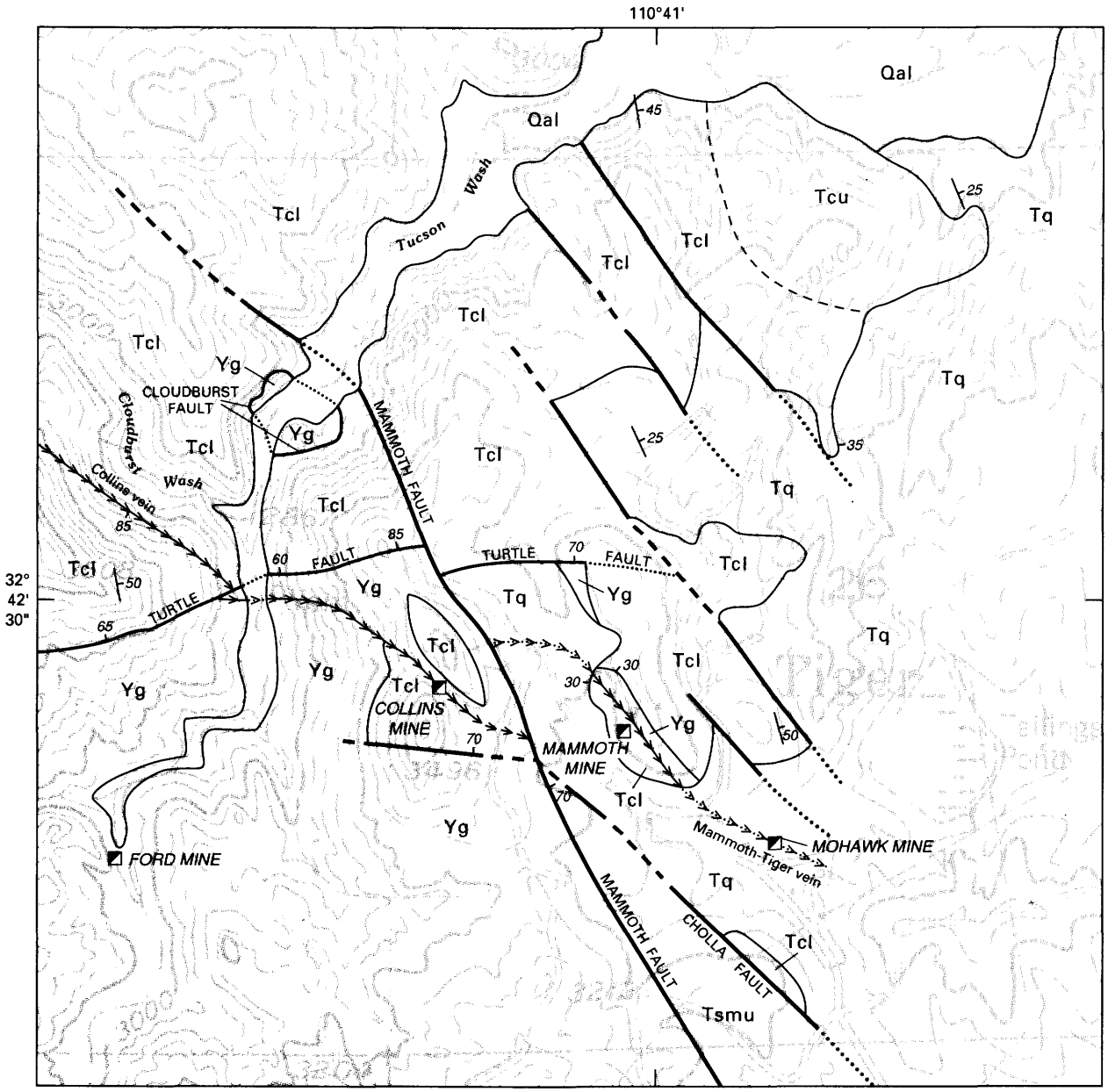

Base from U.S. Geological Survey 1:24,000
Mammoth, 1948 (photorevised 1972)

SCALE 1:12 000

0 500 1000 1500 2000 2500 FEET

0 250 500 750 METERS

CONTOUR INTERVAL 40 FEET

Figure 2. Geologic map of Mammoth area, Arizona. Rhyolite bodies omitted to clarify pre-rhyolite relations; rhyolite shown on plate 1.

with little offset, and thence northwestward high on the bluffs southwest of Cloudburst Wash (up to 3,480 ft or 1,060 m), finally crossing the wash at 3,040 feet or 925 m. Thus the vein south of the Turtle fault shows about 160 m (530 ft) of surface relief, and the vein north of it, about 135 m (440 ft). The host rocks are Oracle Granite and Cloudburst Formation south of the Turtle fault, and entirely Cloudburst Formation north of it. Workings described in the literature are all south of the Turtle fault, but significant effort has clearly been expended on working the northern portion as well.

Rhyolite

The veins of the Collins segment, like the Mammoth-Tiger segment, are closely associated with a swarm of rhyolite bodies on both sides of the Turtle fault (pl. 1). The rhyolite is of course intrusive where Oracle Granite is the host rock, but in Cloudburst host rocks it appears to be both intrusive and extrusive. Most of the clearly extrusive rhyolite bodies have the characteristic stratigraphy and structure of welded tuff, and are concordant to bedding in conglomerate of the Cloudburst Formation. Rhyolite bodies at a high angle to extrusive rhyolite bodies must be intrusive, yet beds of conglomerate above such intrusive rhyolite bodies characteristically contain rhyolite cobbles; this suggests that each intrusive rhyolite body vented nearby.

EXPLANATION

Qal	**Quaternary alluvium**
Tq	**Quiburis Formation**
Tsmu	**San Manuel Formation, Tucson Wash Member**
Tcu	**Cloudburst Formation, upper member**
Tcl	**Cloudburst Formation, lower member**
Yg	**Oracle Granite**
————	**Contact**—Showing dip, where known. Dashed where approximately located
————	**Faults approximately contemporaneous with accumulation of Cloudburst Formation**—Showing dip, where known. Dashed where approximately located; dotted where concealed
————	**Faults approximately contemporaneous with accumulation of Quiburis Formation**—Showing dip, where known. Dashed where approximately located; dotted where concealed
50	**Strike and dip of inclined beds**
>>>>>>	**Mammoth vein set**—Showing dip, where known. Dashed where approximately located; dotted where concealed

Figure 2.—Continued

Many of the intrusive rhyolite bodies are recrystallized to muscovite, quartz, and epidote at the expense of feldspar. This alteration was apparently deuteric, as rhyolitic ash-flow tuff beds are not altered in this way. Near the Collins vein segment, intrusive rhyolite contains quartz veinlets that form 10 percent or more of the rock. Each veinlet shows traces of the same zoning morphology shown by the Mammoth vein set on a larger scale. Quartz veining in other host rocks of the main vein does not reach this density. It is likely that cooling rhyolite was the source of silica in the Mammoth vein set; silica was probably released by the reaction:

potassium feldspar+water=muscovite+quartz

Spatial Relation to the Cloudburst Fault

Four outcrops of Oracle Granite surrounded by Cloudburst Formation (pl. 1; fig. 2) were mapped by Creasey (1965), one as a window through the Cloudburst detachment fault. All four outcrops have proved to be such windows and define a regular, very gentle eastward dip on the detachment surface (fig. 4). The detachment slices off steeply dipping conglomerate beds in the Cloudburst Formation. Individual rhyolite bodies are similarly cut off, but without displacing the rhyolite swarm at map scale. Thus rhyolite emplacement, Cloudburst Formation, and movement on both Cloudburst and Turtle faults must all be broadly synchronous.

The Collins vein segment crops out near one window, and using this control point, one can say that the subhorizontal detachment intersects the part of the Collins vein segment north of the Turtle fault at an elevation of about 2,900 to 3,000 ft (about 900 m; fig. 4). This underground portion of the Collins vein is undescribed.

Metamorphism and Alteration

In the area north of the Turtle fault, Cloudburst Formation rocks that host the Collins vein segment are characterized by epidote-chlorite alteration or metamorphism. The consequent induration of the Cloudburst Formation in this area is undoubtedly a reason that some earlier workers considered the Cloudburst to be of probable Laramide age. The alteration in Oracle Granite south of the Turtle fault is difficult to distinguish from older Laramide propylitic alteration associated with the San Manuel deposit.

Two styles of alteration were observed: (1) Regional alteration in which epidote replaces conglomerate matrix and both phenocrysts and groundmass of volcanic rocks. Epidote also partly fills fractures and vesicles, accompanied by calcite. Such alteration occupies lower elevations in the Cloudburst Formation through much of the block occupied by the Collins vein segment. That is, the upper limit of this alteration is a gently dipping plane. (2) More local alteration in the immediate vicinity of the Collins

vein segment, where Cloudburst Formation host rocks are saturated with epidote and chlorite; fractures and vesicles are generally filled completely. Associated veinlets are quartz and minor adularia rather than calcite. A marginal zone shows manganese oxides and (or) barite on joint surfaces. This style of alteration extends only about 100 m (300 ft) laterally from the Collins vein segment and associated rhyolite. It does not seem to project structurally upward any farther than the first style of alteration; that is, the wallrocks of the Collins segment lack epidote where the vein crosses hills higher in elevation than about 3,100 feet (945 m).

The first style of alteration probably reflects high local geothermal gradients and fluid movement induced by tectonic denudation on the Cloudburst detachment fault where it is present at depths of 100 m (300 ft) or less (fig. 4). The second probably represents heat and fluid transport laterally from the vein system, which acted as a conduit. Cooling rhyolite and other shallow intrusions into the Cloudburst Formation are probably a source of heat for both styles of alteration.

Vein and Wallrock Geology

The Collins segment of the Mammoth vein set strikes about N. 40° to 50° W. and dips about 70° to the southwest; variations in attitude are shown in detail by Peterson (1938). Mineralization is stronger where strike is more northerly. The subsidiary Collins East vein (not mapped) dips steeply northeast (fig. 5), and the projected intersection with the main Collins segment plunges gently southeast.

New exposures of the Collins vein segment are a result of open-pit silica mining in the area of the old Collins mine, on a hilltop at an elevation of about 3,300 to 3,400 feet (about 1,020 m). Detailed maps in Peterson (1938) are a poor guide to these exposures, partly because his study predated open-pit mining and relied on underground and natural-outcrop information, and partly because his rock identifications were faulty. Peterson used "intrusive breccia" and "volcanic" units, which respectively correspond, only approximately, with the rhyolite-clast conglomerate lithology of the Cloudburst Formation and with undifferentiated Cloudburst Formation including both volcanic

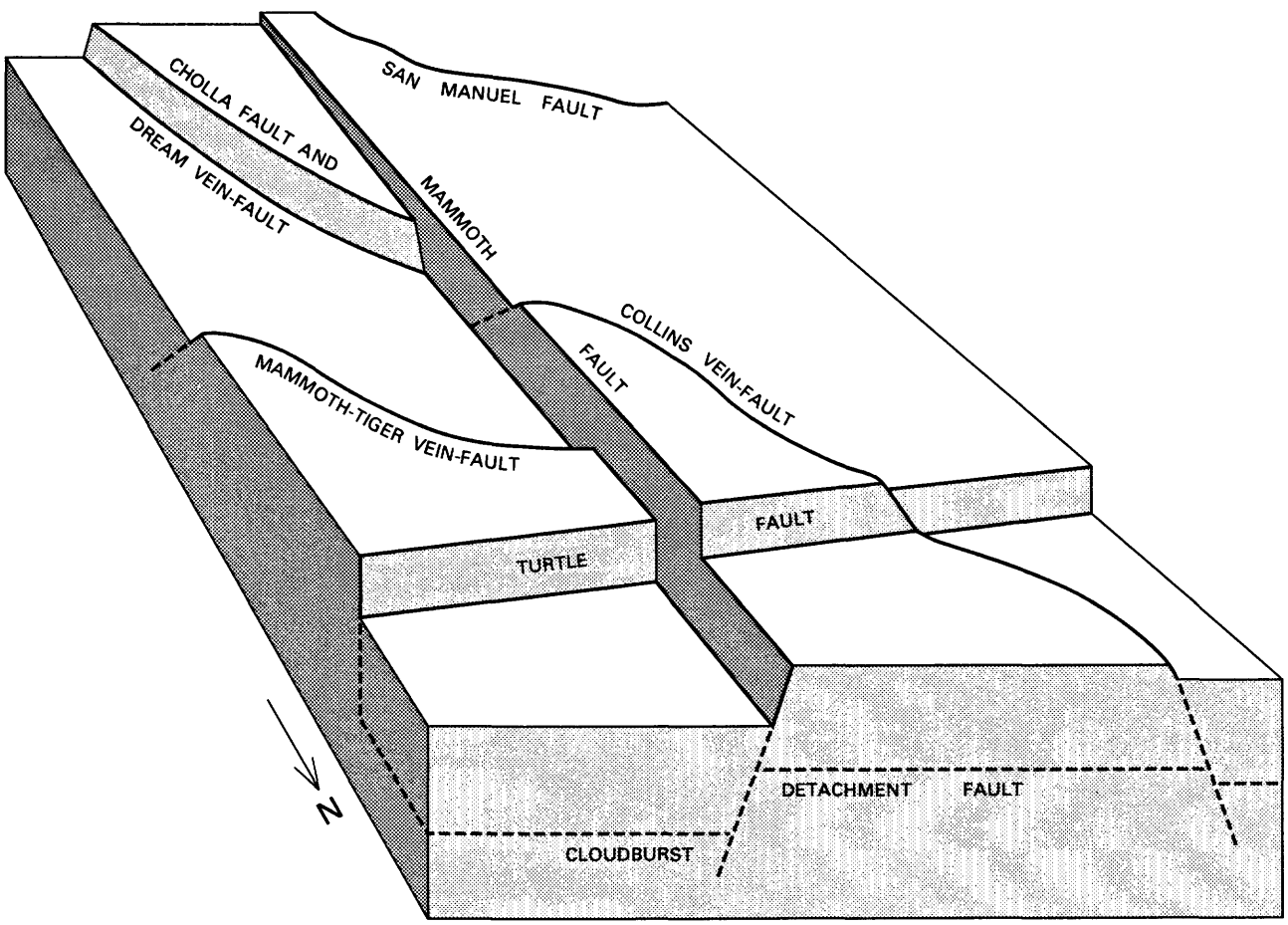

Figure 3. Block diagram of faults in area of Mammoth vein set, viewed from northeast, using arbitrary horizontal datum. Separation magnitude schematic, especially for Turtle fault. For movement on Dream vein-fault, see figure 5.

rocks and volcanic-clast conglomerate. Creasey (1950) first recognized the detrital nature of Peterson's intrusive breccia.

The new exposures of the Collins vein show a gently east-dipping contact between underlying Oracle Granite and overlying conglomerate of the Cloudburst Formation on the northeast wall of the pit (fig. 2). Both units are transected by younger rhyolite intrusions which have to be mentally extracted to perceive the original relations (as in fig. 2). The elevation of the Oracle-Cloudburst contact at the vein is about 3,360 ft (1,025 m). Small faults repeatedly offset the contact, but it is not repeated structurally upward. These relations are consistent with the contact being an unconformity. The southwest wall consists of Cloudburst Formation and rhyolite entirely, except at the south end where a large block of Oracle Granite is juxtaposed along a steep N. 70° W. structure. The fault into which the vein was emplaced was apparently up-to-the-east, with an interfering structure on the west side. Figure 2 suggests that dip-slip movement was about 35 m (120 ft). A right-lateral component of fault movement is also indicated by greater open-space mineralization on the fault segments that strike most nearly north-south.

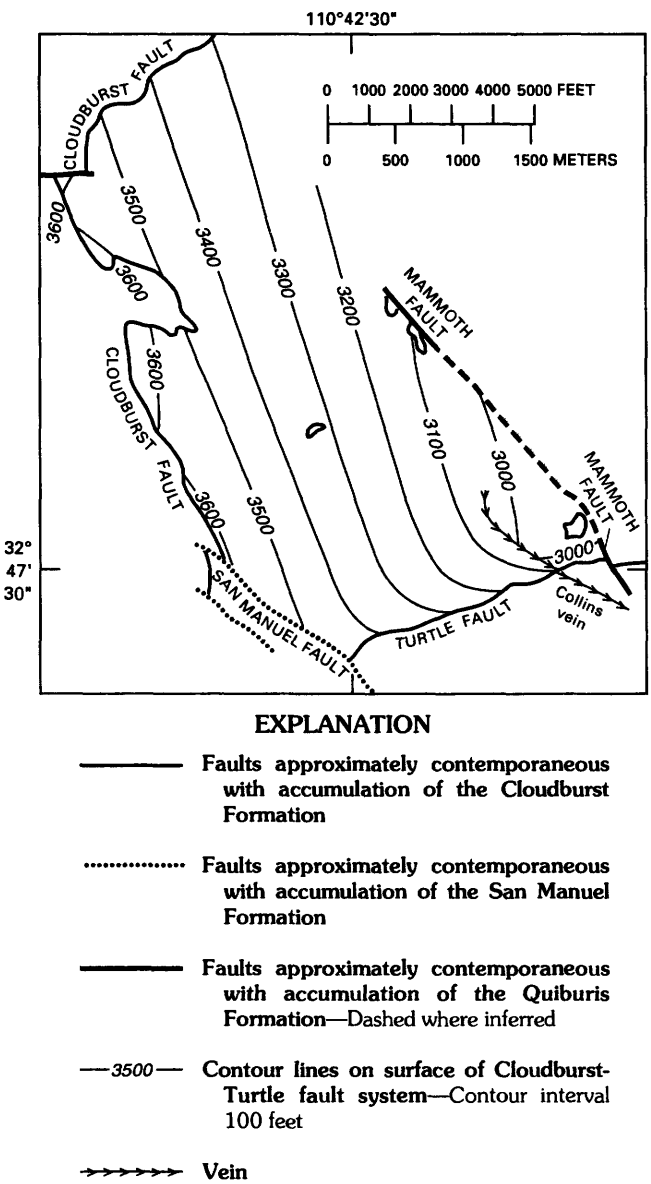

Figure 4. Structure contour map of Cloudburst-Turtle detachment fault system.

Geologic Evolution of the Collins Vein Segment

Rhyolite was emplaced as welded tuffs and very shallow intrusions concurrent with Cloudburst Formation accumulation and faulting on the Turtle and Cloudburst faults. High local geothermal gradients resulted in weak epidote-chlorite metamorphism above the Cloudburst detachment fault. At that time, the Cloudburst detachment probably dipped gently southwestward, and the Cloudburst Formation dipped about 35° to the northeast. Their present attitudes are the result of further northeast tilting (about 25°) on the San Manuel fault system.

The fault into which the Collins vein segment was emplaced cuts the Turtle fault and is largely up-to-the-east. The fault now dips steeply southwest but has been tilted about 25° northeast. Thus it must have formed as a reverse fault. Vein mineralization was concurrent with fault movement. Lateral flow of heat and fluid resulted in

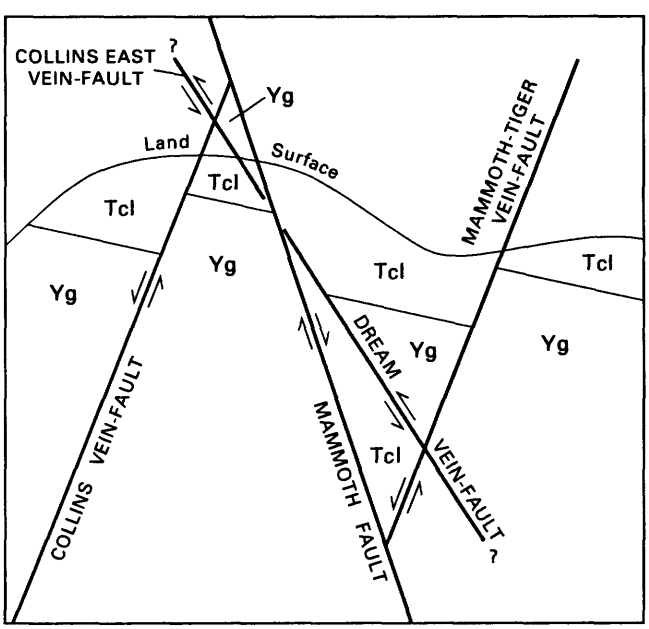

Figure 5. Schematic cross section of the Oracle Granite (Yg)-Cloudburst Formation (Tcl) unconformity in area of Mammoth vein set, showing offsets on various faults. Lack of apparent offset of Collins East and Dream vein-faults is due to composite nature of cross-section (that is, these vein-faults nearly parallel the Mammoth fault in dip but not in strike).

an epidote-saturated aureole around the vein, indicating that the geothermal gradient was still high.

The Mammoth-Tiger Vein Segment

The Mammoth-Tiger segment of the Mammoth vein set is east of the Mammoth fault zone. At depth this vein segment is truncated by the Mammoth fault zone (pl. 1, section *B-B'*).

In many ways the surface traces of the Mammoth-Tiger and Collins vein segments are similar. The Mammoth-Tiger vein dips southwest about 70°; mineralization is apparently strongest in the most north-south-striking parts of the vein. At depth the Mammoth-Tiger vein intersects the subsidiary Dream vein (not mapped), dipping northeast 45° to 65° (fig. 5); the intersection plunges gently southeast (Peterson, 1938). The veins are closely associated with rhyolite, mostly intrusive near the veins but locally extrusive in the same crustal block. The Mammoth-Tiger vein segment intersects the Mammoth fault zone south of the Turtle fault (fig. 2). Its host rocks are both Oracle Granite and Cloudburst Formation. Alteration is chloritic but not epidotic in the Cloudburst host rocks of the Mammoth-Tiger vein segment.

As in the Collins vein segment, recent open-pit mining of the Mammoth-Tiger vein segment has clarified relations shown by Peterson (1938). West of the vein-fault, only Cloudburst Formation is exposed, whereas on the east side, Oracle Granite is overlain by Cloudburst Formation conglomerate along a gently east-dipping contact whose elevation at the vein is about 3,200 feet (975 m; fig. 2). Both pit walls are cut by intrusive rhyolite (pl. 1). Peterson (1938) describes the contact in his text (his p. 11), and his plates show it to the south in the subsurface Mohawk mine workings, where "arkose" is shown overlying Oracle Granite. Thus the relations at the Mammoth-Tiger open cut are similar to those in the Collins open cut—the vein-fault is down on the west, and an Oracle-Cloudburst contact is exposed on the east wall of the pit. Exposure of this valuable relation in both cuts is apparently fortuitous. As in the Collins vein segment, the relation of mineralization intensity to strike of vein-faults suggests a component of right-lateral motion.

Reconstruction

Offsets of three local features can be used to reconstruct the Mammoth-Tiger and Collins vein segments across the Mammoth fault zone:

1. The offset of the veins themselves. Peterson's (1938) subsurface data and more generalized information in Creasey (1950) suggest a downdip separation of 260 to 300 m (850 to 1,000 ft) on the plane of the fault, or 230 to 250 m (750 to 820 ft) vertically. This is the most precise separation value that was available, although it could be a result of various combinations of dip-slip and strike-slip motion. The vein intersections rake rather steeply eastward down the fault plane (fig. 6), and apparent offset at the surface is left-lateral.

2. Apparent offset of the Turtle fault, which dips steeply northwest. The Turtle fault juxtaposes Oracle Granite against Cloudburst Formation near and on both sides of the Mammoth fault zone. Apparent offset is small but in a right-lateral sense, that is, opposite to the veins.

3. If the Dream and Collins East veins (fig. 5) correlate, their intersections with the Mammoth-Tiger and Collins vein segments, respectively, define lines that intersect the Mammoth fault zone (fig. 6). We are apparently first to suggest this correlation.

Figure 6 is an orthogonal view of the plane of the Mammoth fault zone, showing intersections of the above features. Attitudes of these intersections were derived from stereographic projections (not shown). The main veins and the Turtle fault together define a vector that is straight down-dip, with offset of 265 m (875 ft). The intersection of the Dream and Collins East veins with the main veins gives a downdip offset of 262 m (860 ft) with very slight left-lateral motion. These two measures of fault movement differ by only 2 percent in magnitude and 3° in direction, supporting both dip-slip movement and correlation of Dream and Collins East veins. Fault movement apparently dropped the Mammoth-Tiger vein segment from a former position atop the Collins segment (fig. 7).

The Oracle-Cloudburst unconformity on the east walls of the vein-faults shows very little offset; that is, the unconformity has not behaved like the younger datum plane shown in figure 3 along the Mammoth fault zone. This suggests that the Dream vein-fault, older than the Mammoth fault zone, must have had several hundred feet of up-to-the-east movement (fig. 5). This in turn would explain the abrupt change (described above) in apparent dip-slip separation on the younger Cholla fault; the Dream vein-fault and the Cholla fault share virtually the same plane in this area.

Reconstruction as shown in figure 7 implies that the two segments of the Mammoth vein set formed a once-continuous vein set about 550 m (1,800 ft) deep. An additional 640 m (2,100 ft) now eroded would have separated the portion still in the ground from the San Manuel fault system.

The reconstructed vein shows a remarkable gradient in mineral assemblage, complicated by the presence of two horizons of weathering. We suspect, however, that true weathering is a relatively minor factor, as both vein segments show fresh wallrock and lack weathered sulfides within 10 m (30 ft) of the ground surface.

The reconstructed mineral zonation (fig. 7) is derived mostly from descriptions of the separate segments by

Peterson (1938) and Creasey (1950). The economic mineral assemblage of the veins is oxide-dominated except for the deepest 60 m (200 ft), where lead and zinc show their maximum concentrations as sulfides. At shallower depths, lesser lead and zinc are present as carbonates. Molybdenum and vanadium values reach maxima at 60 to 400 m (200 to 1,300 ft) above the deepest levels of mineralization as the oxides wulfenite and vanadinite, respectively. These constituents are virtually absent at deeper levels. Copper, as carbonate and silicate minerals, shows a maximum at 180 m (600 ft) above the lowest level, but lesser copper sulfide increases downward. Gold distribution is irregular and may indeed be controlled by post-faulting redistribution. Peterson noted that the zonation outlined above is present along the strike of the veins also, such that the solutions seem to be derived from deep under the northwest end of the Collins vein segment.

THE SHULTZ SPRING ALTERED ZONE

A narrow area elongated northwest-southeast is altered and weakly mineralized in and north of Tucson Wash, near Shultz Spring, on the upper plate of the San Manuel fault system (fig. 8). This alteration is previously undescribed. Conglomerate of the upper member of the Cloudburst Formation is the host rock. The overlying San Manuel Formation nearby is unaltered, so the alteration is apparently mid-Tertiary.

Alteration

Alteration and mineralization in the Shultz Spring area are disseminated. A continuous set of veins is not present, though some quartz veining occurs. Alteration of

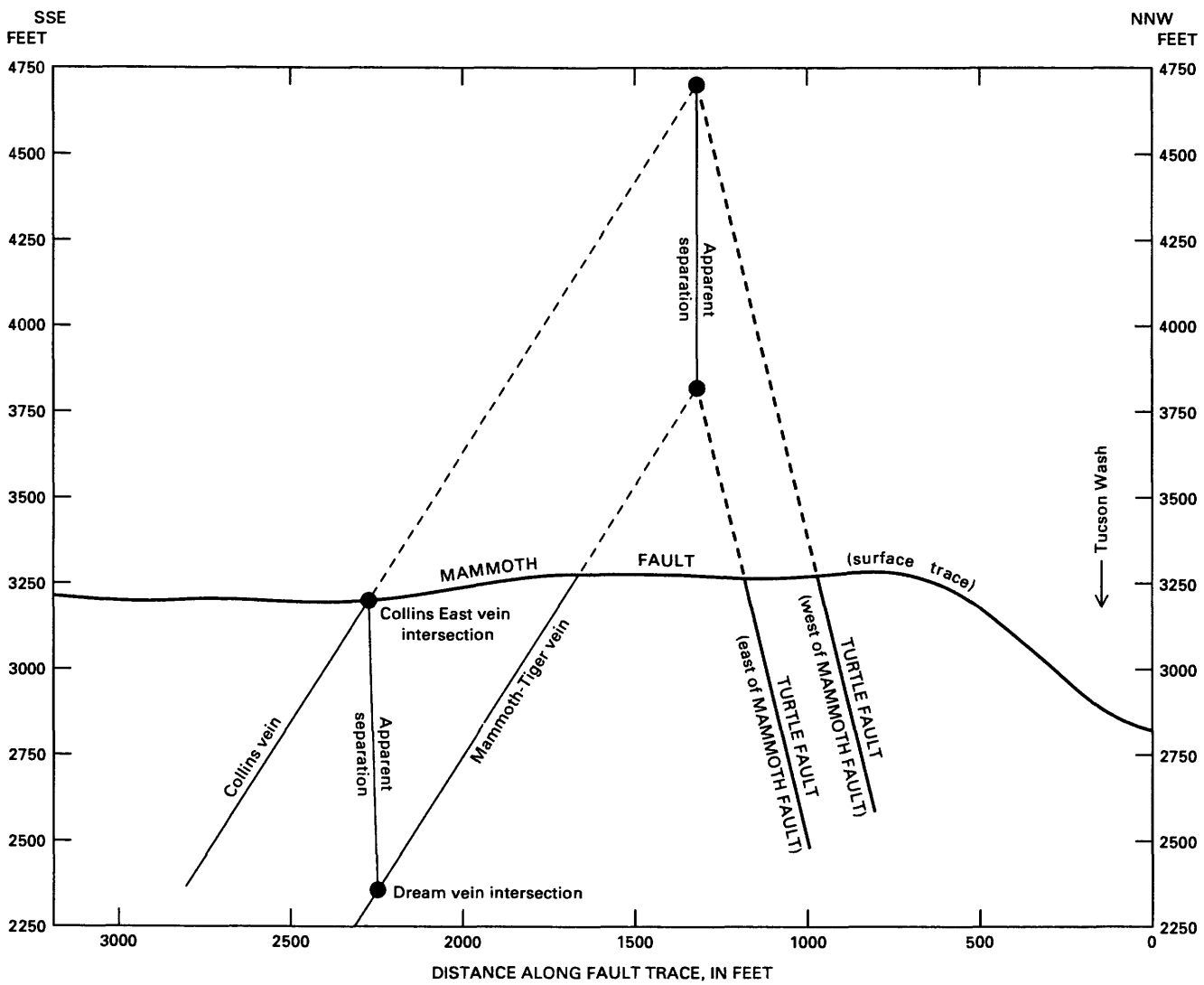

Figure 6. Orthogonal view of Mammoth fault zone, showing vectors derived from offset features.

three types was recognized: (1) change of conglomerate matrix color from red to green, reflecting the recrystallization of finely divided hematite to coarser specular hematite plus chlorite, (2) further recrystallization of matrix to assemblages including specular hematite and locally potassium feldspar, leading in some fine conglomerates to black matrix, and (3) formation of pyrite in conglomerate matrix, and replacement by pyrite of the rims of Oracle Granite cobbles, leading to rusty conglomerate in weathered outcrops. Some of the freshest outcrops, as at Shultz Spring, still contain pyrite. Joints contain barite in type 3 and manganese oxide both in type 1 and the unaltered conglomerates adjacent to it.

Only two alteration zones could be delineated in figure 8; types 1 and 2 were combined. The zones form a roughly concentric pattern. We have no subsurface information with which to extend the zones in three dimensions, though variations with elevation indicate that the pyrite zone becomes stronger at depth.

The tuff unit (Tcut) of Weibel (1981) passes through the altered area (fig. 8) and is itself party altered to carbonate and potassium feldspar. Weibel's potassium feldspar date of 22.5 Ma on this tuff is probably partially reset by this alteration.

Alteration in the Shultz Spring area shows approximately 115 m (380 ft) of topographic relief, from 3,200 to 3,580 feet (975 to 1,090 m) in elevation. Cross-section *B-B'* (pl. 1) suggests that depth to the San Manuel fault system varies from about 185 to 425 m (600 to 1,400 ft).

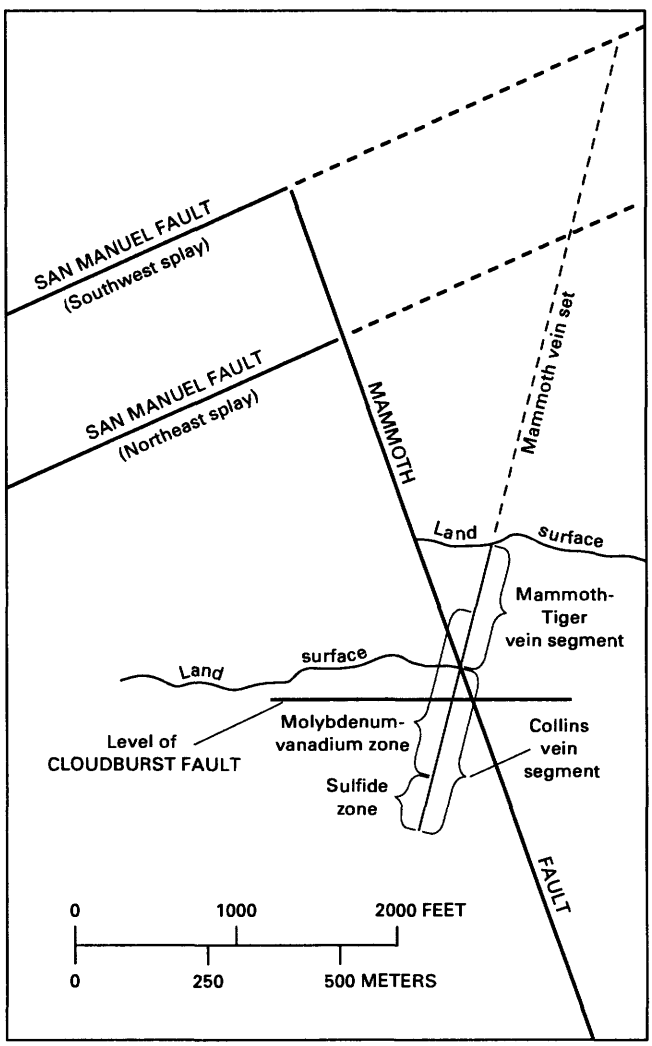

Figure 7. Reconstruction of Mammoth vein set across Mammoth fault zone, looking northwest along section B-B' (pl. 1), showing distribution of mineralization type and probable location of Cloudburst detachment fault (north of Turtle fault only). Dashed lines represent projections of vein set and faults.

Surface Geochemistry of the Shultz Spring Area

A reconnaissance survey of surface geochemistry was conducted as a means of characterizing the mineralization of the Shultz Spring area. A weak but well-centered anomaly of barium, silver, molybdenum, lead, and bismuth was found.

Methods

A 1.6-km (1 mi)-long traverse across the area of altered Cloudburst Formation (fig. 8) was plotted north of and parallel to Tucson Wash. Soil and rock samples were collected approximately every 100 m (330 ft) along the traverse. A total of 17 soil samples were collected at 10 to 15 cm (4 to 6 in.) beneath the ground surface; 21 rock samples were collected from outcrops found both along and south of the traverse (fig. 9). The soil and rock samples are underlain by seven adjacent drainage basins located mostly west of the San Manuel fault system. Each basin covers approximately 0.2 km^2 (0.1 mi^2) of area and contains a central intermittent stream, nearly 0.5 km (0.3 mi) long, which drains into Tucson Wash. At the mouth of each drainage approximately 150 grams (5 oz) of silt-sized stream-sediment was collected near the middle of the dry stream bed and approximately 12 kg (26 lb) of dry silt to sand-sized sediment were collected where magnetite was seen. The bags of sediment were later panned to obtain a heavy-mineral panned concentrate sample for each basin, with the exception of the smallest, basin 7. An additional stream-sediment sample was collected in basin 4 about 0.2 km (0.1 mi) upstream from the sample collected at the mouth. Thus a total of eight stream-sediment and six heavy-mineral panned concentrate samples were obtained (fig. 9). In addition, four stream-sediment and three heavy-mineral panned concentrate samples were collected from four drainage basins east of the San Manuel fault system, 1 km (0.6 mi) west of the Collins segment of the Mammoth vein set. These samples are approximately 1.7 km

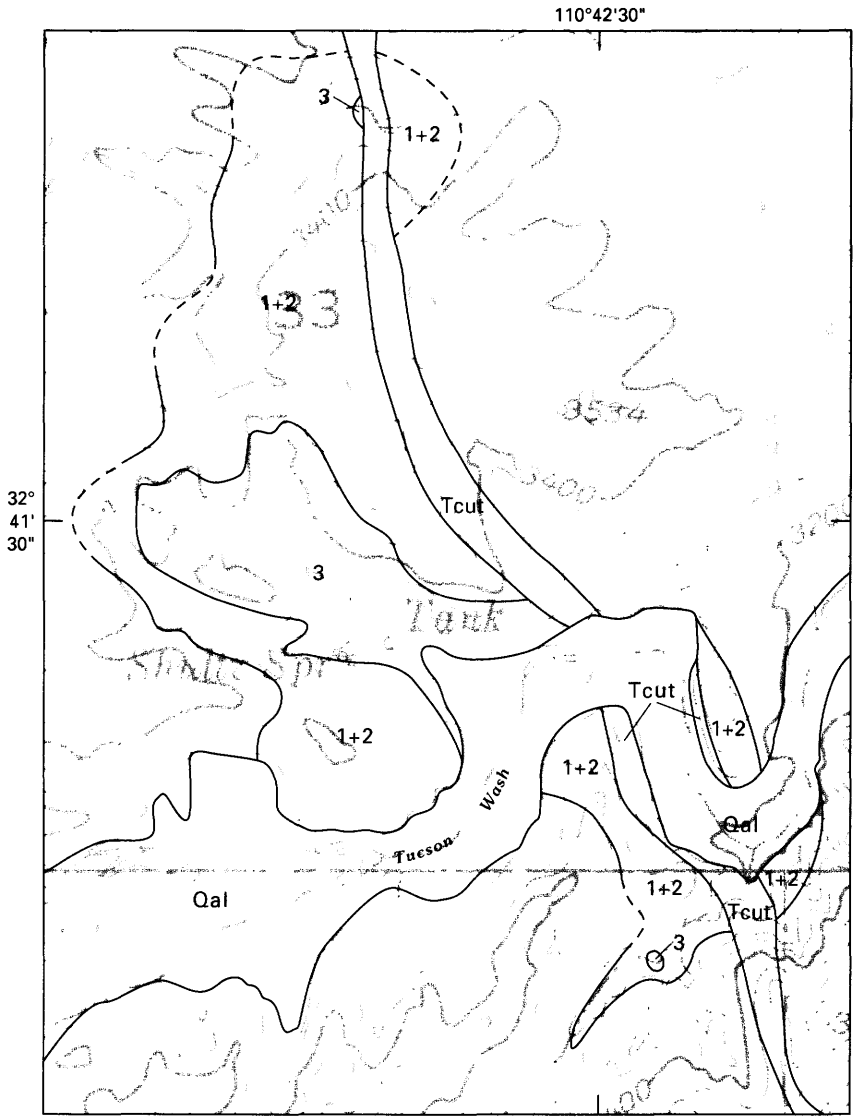

Base from U.S. Geological Survey 1:24,000
Mammoth, 1948 (photorevised 1972)

SCALE 1:12 000

0 500 1000 1500 2000 2500 FEET

0 250 500 750 METERS

CONTOUR INTERVAL 40 FEET

EXPLANATION

——— **Contact**—Between geologic units and/or alteration zones; dashed where approximately located

1+2 **Alteration types 1 (green matrix) and 2 (specular hematite), undivided**

3 **Alteration type 3 (pyrite)**

Figure 8. Map of alteration intensity zones in Shultz Spring area, Arizona. Geologic units except Quaternary alluvium (Qal) and tuff (Tcut) of Cloudburst Formation (Weibel, 1981) omitted (see pl. 1).

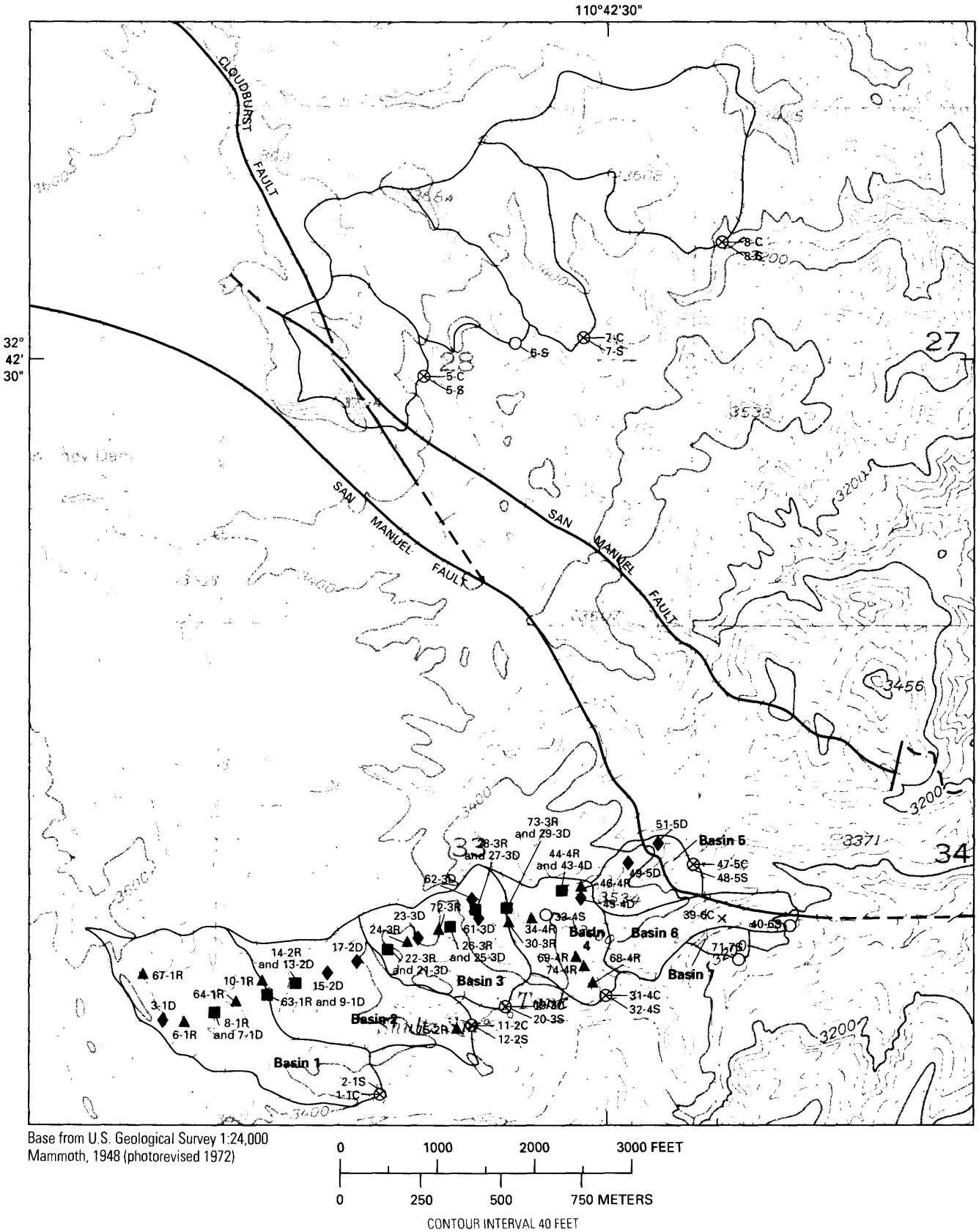

Base from U.S. Geological Survey 1:24,000
Mammoth, 1948 (photorevised 1972)

0 1000 2000 3000 FEET

0 250 500 750 METERS

CONTOUR INTERVAL 40 FEET

Figure 9. Rock, soil, stream-sediment, and heavy-mineral panned concentrate sample and drainage-basin localites. Numbers adjacent to sample localities referred to in text and table 2.

(1 mi) northeast of the samples collected in the Shultz Spring area and allow some comparison between samples from Cloudburst Formation on the lower and upper plates of the San Manuel fault system.

All samples were submitted to the U.S. Geological Survey, Denver, Colo., for sample preparation and analyses by two techniques: the six-step DC-ARC emission-spectrographic method for 35 elements (analyst: R. Hopkins) and the graphite-furnace atomic-absorption method for gold (analyst: B. Roushey). For the panned-concentrate samples, only the nonferromagnetic, minus 35-mesh fraction was analyzed. The results of the analyses are presented in table 2.

The following elements were not detected in any rock, soil, stream-sediment, or panned concentrate samples by the emission-spectrographic method at the detection limits given in parts per million (ppm) in parentheses after the element (the second, higher number is the detection limit for pan concentrated samples only): arsenic (200, 500), gold (10, 20), cadmium (20, 50), germanium (10, 20), and antimony (100, 200). In general, the detection limits for bismuth (10), thorium (100), tin (10), tungsten (20), and zinc (200) were also too high to be useful in this study.

The reliability of the analytical data is of course a major factor in its use. Although some of the analytical data presented here are probably not adequate for detailed geochemical work, they are believed to be useful as a reconnaissance tool to differentiate areas with anomalous metal concentrations from those containing only background concentrations.

For elements with sufficient unqualified data the background values, the mean plus-or-minus two standard deviations, are calculated using the values reported for 12 unaltered rock and 8 unaltered soil samples. Lower limits of anomalous concentration data, the thresholds, were also established (table 3). For elements that have insufficient unqualified data to calculate the mean, any detected occurrence, including values qualified with "L", is considered anomalous where the detection limit of the method greatly exceeds their average crustal abundances. For gold values determined by the atomic-absorption method, any detected occurrence, excluding L.002, is considered anomalous. The thresholds established for soil samples in table 3 are also used to determine the anomalous stream-sediment sample data. Histograms (not shown) were drawn for the heavy-mineral panned concentrate data and the highest separate values are considered anomalous.

EXPLANATION

Sample locality—Numbers referred to in table 2

▲ Rock

◆ Soil

■ Rock and soil

○ Stream sediment

× Heavy-mineral panned concentrate

Drainage basin—Numbers referred to in text and tables

San Manuel and Cloudburst faults—Dashed where inferred

Figure 9.—Continued

Distribution of Anomalous Data in the Shultz Spring Area

Barium

The highest concentrations of barium are found to be roughly coincident with the zone of mapped mineralization which occupies most of basin 3 (table 4; figs. 8, 9, and 10). All soil samples collected in basin 3 contain amounts of barium at threshold (1,500 ppm) or greater (table 3).

Silver

Four of the five samples which contain detectable silver are also located within basin 3 (fig. 11). The silver-bearing samples have high amounts of barium (fig. 10) as well as low amounts of calcium (fig. 12). Three of the high barium-silver rock samples (samples 26-3R, 28-3R, and 22-3R, fig. 9, table 2) are characterized by white to pale yellowish orange (N9 to 10YR 8/6 of Munsell system of color identification (Goddard and others, 1984)) clay alteration. These altered rocks contain low amounts of calcium, magnesium, sodium, cobalt, manganese, and strontium in comparison to unaltered rocks collected from basin 1 (table 5).

Lead

Whereas as much as 15,000 ppm lead is found in heavy-mineral panned concentrate samples collected from drainage basins on the lower San Manuel plate to the east, values of ≤200 ppm lead occur in the Shultz Spring area. However, two of the three samples containing anomalous concentrations of lead in the Shultz Spring area lie within basin 3 (fig. 13).

Bismuth

Fifty ppm bismuth was found in one sample: the heavy-mineral panned concentrate sample from basin 3 (fig. 13).

Molybdenum

All rock, soil, and stream-sediment samples with detectable (≥5L ppm) molybdenum are located in the central

Table 2. Results of analyses of 12 stream-sediment, 9 heavy-mineral panned concentrate, 17 soil, and 21 rock samples from near Tucson Wash in the San Manuel mining district, Arizona

[Analyses by semiquantitative emission spectrography, except for gold which was by atomic absorption. All values in parts per million except for calcium, iron, magnesium, sodium, phosphorous, and titanium, which are in weight percent. Symbols used: <, less than value shown; >, greater than value shown; N, not detected. See figure 9 for sample localities]

Stream sediment samples

Sample	Ca	Fe	Mg	Na	P	Ti	B	Ba	Be	Co	Cr	Cu	Ga
2-1S	1.0	10	.7	1.5	<.2	.7	10	700	2.0	20	150	70	30
12-2S	.5	20	.3	.3	<.2	.7	N	1,500	2.0	30	300	70	50
20-3S	.5	7	.7	1.0	.2	.5	15	2,000	3.0	20	70	200	30
32-4S	.7	15	.5	.5	<.2	.7	N	1,500	1.5	30	300	150	50
33-4S	.7	7	1.0	1.0	.2	.7	30	1,000	3.0	20	100	150	30
48-5S	2.0	5	1.5	2.0	<.2	.5	20	700	3.0	20	150	200	30
40-6S	.7	15	.7	.7	N	1.0	N	500	1.5	30	500	500	30
71-7S	.7	15	.7	.7	N	1.0	N	500	<1.0	30	500	300	30
5-S	1.5	5	1.5	2.0	<.2	.5	20	1,000	3.0	20	150	300	50
6-S	1.5	7	1.5	1.5	N	.7	<10	1,000	1.0	20	200	150	30
7-S	1.5	7	1.5	1.5	<.2	.5	10	1,000	2.0	20	150	300	50
8-S	1.5	5	1.5	1.5	<.2	.5	15	1,500	3.0	20	100	300	30

Sample	La	Mn	Mo	Nb	Ni	Pb	Sc	Sr	V	Y	Zn	Zr	Au
2-1S	70	1,000	N	20	30	70	10	150	300	150	N	1,000	.002
12-2S	20	500	N	<20	30	70	10	N	300	300	N	>1,000	<.002
20-3S	70	700	N	20	30	70	10	200	150	150	N	1,000	<.002
32-4S	150	1,000	N	<20	30	70	10	100	300	300	N	>1,000	<.002
33-4S	70	700	<5	20	30	70	10	300	150	150	N	700	<.002
48-5S	50	1,000	N	<20	50	100	15	300	150	70	N	300	<.002
40-6S	100	1,000	15	20	50	70	10	200	200	200	N	>1,000	.004
71-7S	100	1,500	N	30	30	70	10	200	200	200	N	>1,000	<.002
5-S	50	1,500	N	<20	50	70	15	300	150	30	N	150	.004
6-S	100	1,500	7	20	50	50	15	300	200	50	N	200	.002
7-S	70	1,500	7	20	50	70	15	500	150	30	N	200	.006
8-S	50	2,000	N	<20	30	300	15	300	150	30	<200	150	.004

Table 2. Results of analyses of 12 stream-sediment, 9 heavy-mineral panned concentrate, 17 soil, and 21 rock samples from near Tucson Wash in the San Manuel mining district, Arizona—Continued

Heavy-mineral panned concentrate samples

Sample	Ca	Fe	Mg	Na	P	Ti	B	Ba	Be	Bi
1-1C	7	1.5	.30	.5	5.0	2.0	<20	>10,000	<2	N
11-2C	5	5.0	.30	.5	1.0	2.0	<20	>10,000	<2	N
19-3C	5	.7	.15	N	2.0	2.0	N	>10,000	<2	50
31-4C	7	.7	.15	N	3.0	>2.0	<20	>10,000	N	N
47-5C	15	1.0	.30	<.5	10.0	>2.0	20	500	N	N
39-6C	7	1.0	.30	.5	3.0	>2.0	<20	1,500	N	N
5-C	>50	1.0	.50	<.5	<.5	.7	N	10,000	N	N
7-C	7	2.0	1.00	1.5	.5	>2.0	<20	7,000	<2	N
8-C	30	1.0	.30	<.5	1.5	2.0	<20	>10,000	N	N

Sample	Co	Cr	Cu	Ga	La	Mn	Mo	Nb	Ni
1-1C	N	20	20	<10	100	700	N	<50	N
11-2C	N	50	N	10	<100	500	N	50	N
19-3C	N	<20	N	<10	<100	500	N	50	N
31-4C	N	20	N	<10	<100	500	N	<50	N
47-5C	N	70	70	10	100	500	N	50	<10
39-6C	N	50	50	<10	100	500	N	<50	N
5-C	<20	30	50	N	<100	500	N	50	N
7-C	N	100	200	15	<100	700	150	70	<10
8-C	N	50	200	N	100	700	700	50	N

Sample	Pb	Sc	Sn	Sr	Th	V	W	Y	Zr	Au
1-1C	70	150	N	500	N	150	N	1,000	>2,000	N
11-2C	70	100	N	1,500	N	100	N	700	>2,000	N
19-3C	200	70	N	2,000	200	150	N	700	>2,000	N
31-4C	70	200	N	700	200	200	N	1,500	>2,000	N
47-5C	100	150	N	N	N	200	N	1,500	>2,000	.0
39-6C	70	200	N	N	<200	200	N	1,000	>2,000	17.120
5-C	200	30	N	500	N	150	N	700	>2,000	.0
7-C	3,000	70	30	500	N	700	N	200	>2,000	.0
8-C	15,000	70	N	1,500	N	3,000	300	500	>2,000	.0

Table 2. Results of analyses of 12 stream-sediment, 9 heavy-mineral panned concentrate, 17 soil, and 21 rock samples from near Tucson Wash in the San Manuel mining district, Arizona—Continued

Rock samples

Sample	Ca	Fe	Mg	Na	P	Ti	Ag	B	Ba	Be	Co	Cr	Cu
67-1R	.30	3	.70	2.0	<.2	.30	.5	15	1,500	2.0	15	50	30
6-1R	2.00	3	1.50	3.0	<.2	.20	N	15	1,500	1.5	15	100	30
8-1R	2.00	3	.70	2.0	<.2	.20	N	20	1,000	1.5	15	50	20
64-1R	5.00	5	1.00	2.0	N	.30	N	20	1,000	2.0	20	100	20
10-1R	.70	3	1.50	1.5	<.2	.30	N	20	1,000	1.5	20	70	30
63-1R	2.00	3	1.00	2.0	<.2	.30	N	30	700	1.5	15	30	20
14-2R	7.00	3	.70	1.5	N	.20	N	30	1,000	2.0	15	20	20
75-2R	.15	3	.30	1.5	<.2	.30	N	20	1,000	3.0	<10	<10	10
22-3R	.20	2	.30	.7	.2	.20	<.5	15	>5,000	2.0	<10	20	30
24-3R	.30	3	.50	1.0	<.2	.30	N	20	>5,000	1.5	10	20	20
26-3R	.15	2	.50	N	N	.50	<.5	30	1,500	1.5	N	30	10
72-3R	.20	3	.30	.7	N	.20	N	15	2,000	2.0	50	20	20
28-3R	.15	3	.30	1.0	<.2	.30	N	20	1,500	3.0	<10	15	30
30-3R	.70	2	.15	2.0	<.2	.15	N	70	2,000	3.0	<10	30	30
73-3R	.30	3	.30	2.0	.2	.20	<.5	30	1,500	3.0	N	20	20
34-4R	10.00	3	.70	2.0	<.2	.15	N	20	1,000	3.0	10	30	20
68-4R	10.00	3	.70	2.0	N	.20	N	15	1,000	2.0	10	30	20
69-4R	1.50	3	.70	1.0	N	.30	N	30	700	3.0	20	30	20
74-4R	5.00	3	.70	1.5	<.2	.30	N	20	700	2.0	15	20	20
44-4R	5.00	2	.50	2.0	N	.20	N	30	1,000	3.0	15	15	20
46-4R	3.00	3	1.50	1.5	N	.30	N	20	1,500	1.5	30	100	30

Sample	Ga	La	Mn	Mo	Nb	Ni	Pb	Sc	Sr	V	Y	Zn	Zr
67-1R	30	50	500	N	20	30	70	15	200	100	50	N	300
6-1R	30	50	700	N	<20	30	50	7	300	70	30	N	200
8-1R	30	<50	700	N	N	20	30	7	200	100	10	N	100
64-1R	30	50	1,000	N	20	30	70	15	300	100	70	<200	200
10-1R	30	<50	700	N	20	30	50	15	150	100	50	<200	200

Table 2. Results of analyses of 12 stream-sediment, 9 heavy-mineral panned concentrate, 17 soil, and 21 rock samples from near Tucson Wash in the San Manuel mining district, Arizona—Continued

63-1R	30	<50	700	N	<20	20	30	7	300	100	15	<200	100
14-2R	30	<50	1,500	N	<20	10	50	7	300	70	50	N	150
75-2R	20	<50	100	N	<20	5	30	10	N	70	20	300	100
22-3R	15	<50	150	N	<20	<5	50	7	300	70	30	N	200
24-3R	15	<50	500	N	<20	10	50	10	700	70	30	N	300
26-3R	30	70	150	N	20	<5	30	10	N	100	30	N	200
72-3R	20	<50	2,000	15	<20	30	50	7	N	70	30	N	150
28-3R	20	<50	200	N	<20	<5	50	7	<100	70	30	N	200
30-3R	20	<50	700	20	30	<5	70	7	N	50	70	N	150
73-3R	20	<50	700	N	<20	<5	70	10	N	50	50	N	150
34-4R	30	<50	1,000	N	<20	7	50	10	300	50	30	N	100
68-4R	30	<50	1,500	N	<20	10	50	10	<100	70	30	N	100
69-4R	20	50	700	N	20	7	30	10	300	70	50	N	200
74-4R	20	50	1,000	N	<20	5	30	10	300	70	50	N	100
44-4R	20	<50	700	N	<20	7	50	7	200	70	30	N	70
46-4R	30	<50	700	N	<20	50	30	15	1,000	100	30	N	100

Table 2. Results of analyses of 12 stream-sediment, 9 heavy-mineral panned concentrate, 17 soil, and 21 rock samples from near Tucson Wash in the San Manuel mining district, Arizona—Continued

Soil samples

Sample	Ca	Fe	Mg	Na	P	Ti	Ag	B	Ba
3-1D	1.0	5	1.5	1.0	<.2	.5	N	20	700
7-1D	5.0	3	.7	.7	<.2	.3	N	20	700
9-1D	.5	3	1.0	.7	.2	.5	N	20	700
13-2D	1.5	7	1.0	1.5	<.2	.5	N	30	1,000
15-2D	1.5	5	1.0	1.5	<.2	.5	N	30	1,000
17-2D	.7	5	1.0	2.0	<.2	.5	N	30	1,500
21-3D	.7	3	.7	1.0	<.2	.3	.7	30	2,000
23-3D	.7	5	1.0	2.0	<.2	.5	N	30	2,000
25-3D	1.0	3	.7	.7	.3	.3	N	30	2,000
27-3D	.7	5	1.0	1.5	<.2	.5	N	30	2,000
61-3D	1.5	5	1.0	1.5	<.2	.5	N	30	5,000
62-3D	.3	5	.7	1.5	N	.5	N	30	1,500
29-3D	5.0	3	1.0	1.0	1.0	.3	N	50	3,000
43-4D	2.0	3	.7	.7	<.2	.3	N	30	700
45-4D	3.0	3	1.0	1.0	<.2	.3	N	20	700
49-5D	7.0	3	1.5	1.5	N	.3	N	20	700
51-5D	.7	5	1.0	1.5	<.2	.5	N	20	1,000

Sample	Be	Co	Cr	Cu	Ga	La	Mn	Mo	Nb
3-1D	2.0	20	100	50	30	70	1,000	N	20
7-1D	3.0	15	100	50	15	70	700	N	20
9-1D	3.0	15	100	50	15	70	700	N	20
13-2D	2.0	20	150	70	30	70	1,000	N	20
15-2D	3.0	20	150	50	30	70	1,000	N	20
17-2D	2.0	20	100	150	50	100	1,000	<5	20
21-3D	2.0	15	100	70	30	70	500	N	20
23-3D	2.0	20	100	300	30	70	700	7	20
25-3D	3.0	20	70	70	30	70	700	N	<20
27-3D	3.0	20	100	70	30	70	700	N	20

Table 2. Results of analyses of 12 stream-sediment, 9 heavy-mineral panned concentrate, 17 soil, and 21 rock samples from near Tucson Wash in the San Manuel mining district, Arizona—Continued

61-3D	2.0	20	100	100	30	70	700	N	20
62-3D	3.0	20	100	100	30	70	700	N	20
29-3D	3.0	15	70	70	20	70	1,000	<5	20
43-4D	3.0	15	50	50	15	70	700	N	20
45-4D	2.0	15	100	70	15	70	700	N	<20
49-5D	1.5	20	100	50	20	50	700	N	20
51-5D	2.0	20	100	70	30	70	700	N	20

Sample	Ni	Pb	Sc	Sr	V	Y	Zn	Zr	Au
3-1D	50	70	15	100	100	100	<200	500	<.002
7-1D	30	50	15	100	100	50	N	200	N
9-1D	30	50	15	<100	100	50	N	300	<.002
13-2D	50	70	15	150	150	70	N	300	N
15-2D	50	70	15	100	100	70	<200	150	<.002
17-2D	30	70	20	200	150	100	N	300	.002
21-3D	30	70	15	<100	150	70	<200	500	<.002
23-3D	30	100	20	100	150	70	N	500	.002
25-3D	30	70	15	150	150	100	N	500	<.002
27-3D	50	50	20	<100	150	100	N	500	<.002
61-3D	30	70	20	150	150	150	N	500	.006
62-3D	30	70	20	150	150	100	N	700	.002
29-3D	20	50	15	300	100	70	N	150	<.002
43-4D	20	50	15	<100	100	70	N	300	.002
45-4D	30	50	15	300	100	50	N	200	.002
49-5D	30	50	15	300	150	30	N	150	<.002
51-5D	30	70	15	200	100	100	<200	300	.002

Table 3. Summary of statistical data and threshold concentrations of semiquantitative spectrographic data for rock and soil samples without alteration in the Shultz Spring area, Arizona

[All values in parts per million except those for iron, magnesium, calcium, titanium, and sodium, which are in weight percent. L, detected but below limit of determination; --, no data.

Values are reported as 0.15, 0.2, 0.3, 0.5, 0.7, 1.0, or powers of 10 of these numbers that are the rounded values for the approximate geometric midpoints (0.16, 0.22, 0.34, 0.46, 0.73, 1.0, or powers of 10 of these numbers) of the intervals for the six steps per order of magnitude dilution of a standard by one order of magnitude (Motooka and Grimes, 1976). For a calculated background ($\bar{x}+2\sigma$) that falls between the approximate geometric midpoints, the background is taken as the reported value corresponding to the midpoint of the closest value. For example, $\bar{x}+2\sigma$ of lead in rocks is 69 ppm. The number 69 falls closest to 73, which is reported as 70. Thus, the background value for lead is assigned as 70 ppm. The threshold is taken as the adjacent higher reporting interval. Thus the threshold is 100 ppm of lead.

Codes for column "Explanation of Threshold Determination": a, background values not determined; b, only unqualified data used to calculate mean (background ($\bar{x}+2\sigma$) used); c, insufficient unqualified data to calculate $\bar{x}+2\sigma$ (any detected occurrence, including L, considered anomalous)]

Element	Detection limit	Number of samples (n)	Arithmetic mean ($\bar{x}_n$)	Standard deviation (σ)	Background ($\bar{x}+2\sigma$)	Threshold (lower limit of anomalous data)	Explanation of threshold determination	Number of samples (n)	Arithmetic mean ($\bar{x}_n$)	Standard deviation (σ)	Background ($\bar{x}+2\sigma$)	Threshold (lower limit of anomalous data)	Explanation of threshold determination
		Rock Samples						Soil Samples					
Fe	.05	12	3.1	.7	--	--	a	8	4.3	1.5	--	--	a
Mg	.02	12	.9	.4	--	--	a	8	1.1	.3	--	--	a
Ca	.05	12	4.4	3.2	--	--	a	8	2.5	2.3	--	--	a
Ti	.002	12	.2	.1	--	--	a	8	.4	.1	--	--	a
Na	.2	12	1.8	.5	--	--	a	8	1.2	.4	--	--	a
Ag	.5	21	--	--	--	.5L	c	17	--	--	--	.5L	c
As	200	21	--	--	--	200L	c	17	--	--	--	200L	c
Au	10	21	--	--	--	10L	c	17	--	--	--	10L	c
B	10	12	23	6	30	50	b	8	23	5	30	50	b
Ba	20	12	1,000	260	1,500	2,000	b	8	810	160	1,000	1,500	b
Be	1	12	2	1	3	5	b	8	2	1	3	5	b
Bi	10	21	--	--	--	10L	c	17	--	--	--	10L	c
Cd	20	21	--	--	--	20L	c	17	--	--	--	20L	c
Co	5	12	17	5	20	30	b	17	18	3	20	30	b
Cr	10	12	50	34	100	150	b	8	110	23	150	200	b
Cu	5	12	23	4.5	30	50	b	8	51	23	100	150	b
La	20	4	50	0	50	70	b	8	68	7	70	100	b
Mn	10	12	910	310	1,500	2,000	b	8	810	160	1,000	1,500	b
Mo	5	21	--	--	--	5L	c	17	--	--	--	5L	c
Nb	20	3	20	0	20	30	b	7	20	0	20	30	b
Ni	5	12	19	14	50	70	b	8	38	10	50	70	b
Pb	10	12	43	13	70	100	b	8	60	11	70	100	b
Sb	100	21	--	--	--	100L	c	17	--	--	--	100L	c
Sc	5	12	10	3	15	20	b	8	15	0	15	20	b
Sn	10	21	--	--	--	10L	c	17	--	--	--	10L	c
Sr	100	11	330	230	700	1,000	b	7	180	91	300	500	b
Th	100	21	--	--	--	100L	c	17	--	--	--	100L	c
V	10	12	81	18	100	150	b	8	110	23	150	200	b
W	50	21	--	--	--	50L	c	17	--	--	--	50L	c
Y	10	12	37	17	70	100	b	8	65	25	100	150	b
Zn	200	21	--	--	--	200L	c	17	--	--	--	200L	c
Zr	10	12	1	51	200	300	b	8	260	120	500	700	b

Table 4. Concentrations of barium in rock, stream-sediment, heavy-mineral panned concentrate, and soil samples from the Shultz Spring area, Arizona

[Basins are listed as found consecutively from west to east (fig. 9). Concentrations in parts per million. nc; none collected]

Drainage basin	Rock samples	Stream sediments	Heavy-mineral panned concentrates	Soil samples
Basin 1	700-1,500	700	>10,000	700-700
Basin 2	1,000-1,000	1,500	>10,000	1,000-1,500
Basin 3	1,500->5,000	2,000	>10,000	1,500-5,000
Basin 4	700-1,500	1,500	>10,000	700-700
Basin 5	nc	700	500	700-1,000
Basin 6	nc	500	1,500	nc

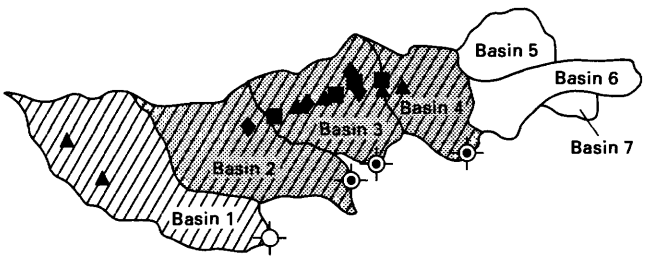

EXPLANATION

Barium concentration, in parts per million

Sample type

- ▲ **2,000 - >5,000 in rock**
- ♦ **1,500 - >5,000 in soil**
- ■ **1,500 - >5,000 in rock and soil**
- **>10,000 in heavy-mineral panned concentrate**
- **1,500 - 2,000 in stream sediment**

Figure 10. Distribution of regionally anomalous values for barium in drainage basins west of San Manuel fault, Ariz. See figure 9 for location.

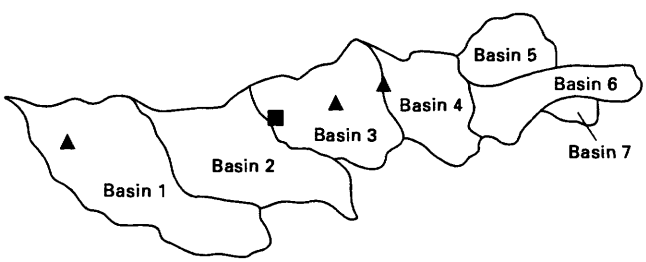

EXPLANATION

Silver concentration, in parts per million

Sample type

- ▲ **≤0.5 in rock**
- ■ **<0.5 and 0.7 in rock and soil, respectively**

Figure 11. Distribution of regionally anomalous values for silver in drainage basins west of San Manuel fault, Ariz. See figure 9 for location.

Table 5. Ranges of concentrations of calcium, magnesium, sodium, cobalt, manganese, and strontium in rocks collected in drainage basins 1 and 3 (fig. 9)

[wt. pct., weight percent; ppm, parts per million; N, not detected; L, detected at less than the spectrographic limit of determination]

	Basin 3 (3 altered rock samples: 22-3R, 26-3R, and 28-3R)	Basin 1 (5 rock samples: 6-1R, 8-1R, 10-1R, 63-1R, and 64-1R)
Calcium	0.15-0.2 wt. pct.	0.30-5.0 wt. pct.
Magnesium	0.30-0.5 wt. pct.	0.70-1.5 wt. pct.
Sodium	N0.2 -0.7 wt. pct.	1.5 -3.0 wt. pct.
Cobalt	N10- L10 ppm	15- 20 ppm
Manganese	150- 200 ppm	500-1,000 ppm
Strontium	N100-L100 ppm	150- 300 ppm

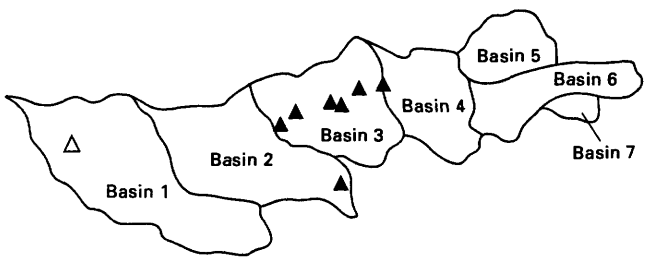

EXPLANATION

Calcium and magnesium concentrations, in weight percent

Sample type

- ▲ **Calcium ≤0.3 in rock**
  Magnesium ≤0.5 in rock
- △ **Calcium 0.3 in rock**

Figure 12. Distribution of regionally anomalous values for calcium and magnesium in drainage basins west of San Manuel fault, Ariz. See figure 9 for location.

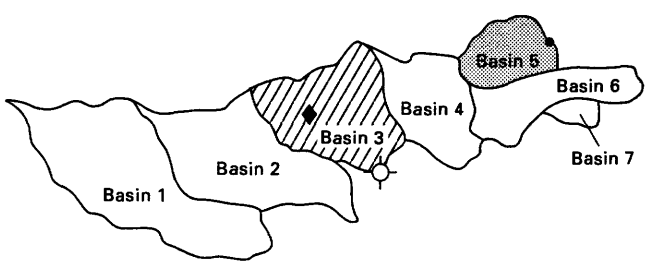

EXPLANATION

Lead and bismuth concentrations, in parts per million

Sample type

- ♦ **100 lead in soil**
- **200 lead and 50 bismuth in heavy-mineral panned concentrate**
- **100 lead in stream sediment**

Figure 13. Distribution of regionally anomalous values for lead and bismuth in drainage basins west of San Manuel fault, Ariz. See figure 9 for location.

mineralized area with the exception of one stream-sediment sample collected from basin 6 (fig. 14). Molybdenum was not detected in heavy-mineral panned concentrate samples.

Gold

No gold in an amount greater than 2 parts per billion (ppb) was detected in any rock sample by the atomic-absorption method. However, 2 to 6 ppb gold were detected in six soil samples located on top of and east of the mineralized zone (fig. 15). Several of these soils are reddish brown (10R 4/6) to dark red (5R 3/6) and overlie Cloudburst Formation conglomerate that ranges from moderate red (5R 5/4) to grayish red (10R 4/2). Four of the gold-bearing soil samples also contain high (1,500 to 5,000 ppm) amounts of barium. Gold was not detected in the stream-sediment and heavy-mineral panned concentrate samples collected downstream from the soil samples containing gold (fig. 15). However, 2 and 4 ppb gold were found in the stream-sediment samples from basins 1 and 6, and 17 ppm gold were found in the heavy-mineral panned concentrate sample collected in basin 6 (fig. 15).

Copper

The distribution of samples with anomalously high amounts of copper (fig. 16; table 3) generally coincides with the distribution of gold-bearing samples (fig. 15). In the mineralized area of basins 3 and 4, stream-sediment samples containing 150 to 300 ppm copper are located downstream from gold-bearing soil samples (figs. 15 and 16). In basin 6, stream-sediment sample 40-6S contains 300 ppm copper and 4 ppb gold, and heavy-mineral panned concentrate sample 39-6C, located about 0.1 mi (0.2 km) upstream from sample 40-6S (fig. 9), contains 50 ppm copper and 17 ppm gold (table 2).

In the Shultz Spring area copper occurs in higher quantities in soil and stream-sediment samples than it does in the heavy-mineral panned concentrate samples (compare 300 and 500 ppm Cu in stream-sediments to 50 and 70 ppm Cu in heavy-mineral panned concentrate samples (table 2)). Probably the copper is adsorbed on fines or occurs in a magnetic mineral in the concentrate (only the

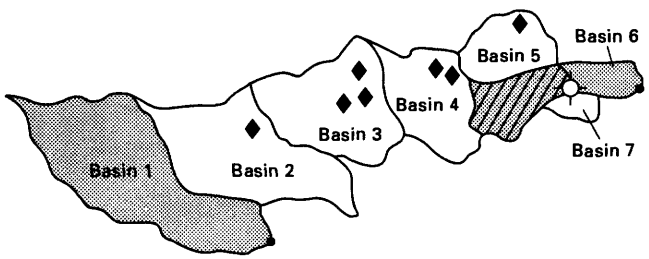

EXPLANATION

Gold concentration, in parts per million (ppm) or parts per billion (ppb)

Sample type

- ♦ **2 - 6 ppb in soil**
- **17 ppm in heavy-mineral panned concentrate**
- **2 - 4 ppb in stream sediment**

Figure 15. Distribution of regionally anomalous values for gold in drainage basins west of San Manuel fault, Ariz. See figure 9 for location.

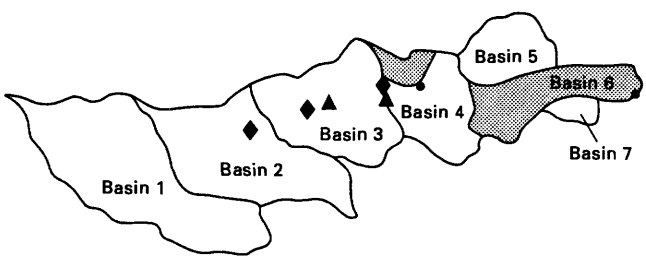

EXPLANATION

Molybdenum concentration, in parts per million

Sample type

- ▲ **15 - 20 in rock**
- ♦ **5L - 7 in soil**
- **5L - 15 in stream sediment**

Figure 14. Distribution of regionally anomalous values for molybdenum in drainage basins west of San Manuel fault, Ariz. L, detected at less than spectrographic limit of determination. See figure 9 for location.

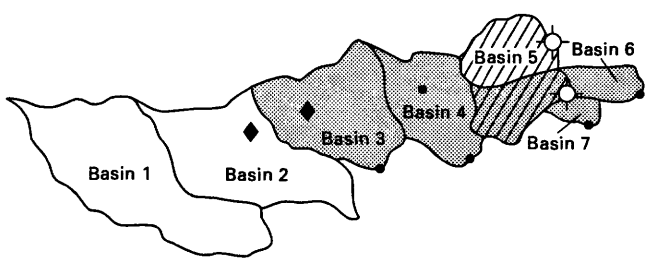

EXPLANATION

Copper concentration, in parts per million

Sample type

- ♦ **150 - 300 in soil**
- **50 - 70 in heavy-mineral panned concentrate**
- **150 - 300 in stream sediment**

Figure 16. Distribution of regionally anomalous values for copper in drainage basins west of San Manuel fault, Ariz. See figure 9 for location.

nonferromagnetic fraction of the heavy-mineral panned concentrate sample was analyzed). Higher values (200 ppm) of copper occur in the heavy-mineral panned concentrate samples east of the San Manuel fault.

Zinc

Zinc-bearing samples are located mostly west of the altered area at Shultz Spring (figs. 8 and 17). Zinc was detected at less than 200 ppm in rock and soil samples in basin 1. Zinc was not detected in the stream-sediment or in the heavy-mineral panned concentrate samples. A white (N9) to pale-yellowish-orange (10 YR 8/6) altered rock containing minor amounts of pyrite was collected at Shultz Spring. This rock contains 300 ppm zinc and is depleted in calcium (0.15 percent) and manganese (100 ppm).

Discussion

A zone characterized by high amounts of barium; low, but detectable, values of silver, lead, molybdenum, gold, and copper; depleted amounts of calcium, manganese, magnesium, sodium, strontium, and cobalt; and a single occurrence of 50 ppm bismuth coincides with the Shultz Spring altered area. Some of the rock and soil samples peripherally located west of the altered area contain low amounts of zinc.

Economic mineralization in the Shultz Spring area may be rather modest considering the impressive amounts of alteration and local pyrite concentrations. The most enriched stream-sediments and concentrates from the Shultz Spring area are not as high in mineral concentrations as samples from an area on the lower plate of the San Manuel fault that does not include the Mammoth vein set (samples 5-S, 5-C, 6-S, 7-S, 7-C, 8-S, and 8-C, fig. 9 and table 2).

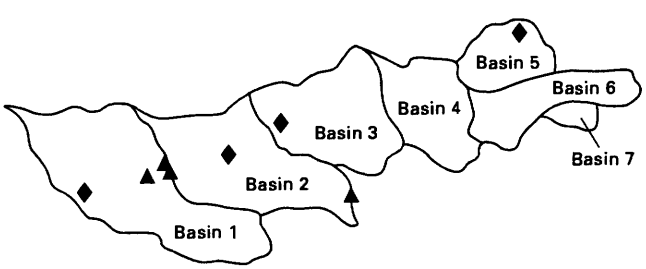

EXPLANATION

Zinc concentration, in parts per million

Sample type

▲ **200L and 300 in rock**

♦ **200L in soil**

Figure 17. Distribution of regionally anomalous values for zinc in drainage basins west of San Manuel fault, Ariz. L, detected at less than spectrographic limit of determination. See figure 9 for location.

Table 6. Attitudes of features used to determine offset on the San Manuel fault

[(P) planes for which strike and dip are listed; (L) line for which trend and plunge are listed]

	Upper plate of San Manuel fault	Lower plate of San Manuel fault
Turtle fault (P)	N. 51° E., 62° NW.	N. 66° E., 62° NW.
Cloudburst-over-Oracle unconformity (P)	N. 41° W., 30° NE.	N. 28° W., 35° NE.
Intersection (L)	N. 35° E., 28° NE.	N. 43° E., 34° NE.

Tectonic Relation to the Mammoth Vein Set

Since both the Mammoth vein set and the Shultz Spring altered area are pre-San Manuel Formation and thus pre-San Manuel fault system, and since the shape and orientation of their altered areas are similar, one might expect that the Shultz Spring area is the faulted upper portion of the Mammoth vein set. If this were so, the offset shown in section *B-B'* (pl. 1) would be 3,475 m (11,400 ft) or more. The fault offset listed by Lowell (1968) is about 2,440 m (8,000 ft) but his figure 3 suggests that the offset may be about 3,050 m (10,000 ft) horizontally, or 3,350 m (11,000 ft) along the fault plane. In view of the resultant uncertain correlation of altered areas, we derived our own vector for total movement on the San Manuel fault system. We used two features whose potential for correlation was not clear in 1968, the Turtle fault and the Oracle-Cloudburst unconformity. These two planar features, present on both upper and lower plates of the San Manuel fault system (table 6), intersect along a line that is offset by the fault. A fault-plane solution (similar to fig. 6) yields a separation magnitude of 2,363 m (7,750 ft), very close to Lowell's value, but in a direction of S. 46° W., or 9° from Lowell's direction of S. 55° W. Our method does not yield an independent estimate of the dip of the fault system.

Our value of separation on the San Manuel fault system suggests that the Mammoth vein set and the Shultz Spring altered area are not the same feature. Quite possibly the entire upper-plate segment of the Mammoth vein set has been eroded away (section *B-B'*, pl. 1). Conversely, the Shultz Spring altered area corresponds (using our new vector) with the Ford (or Thunderbird) mine area (pl. 1; fig. 2) on the lower plate, though uncertainty of the dips makes the correlation tentative. The Ford mine is an altered area with epidotized black dikes, quartz veins, and faults striking N. 10° to 60° W., dipping steeply either east or west. These characteristics are compatible with Shultz Spring alteration zones. If the proposed correlation is correct, the Ford mine alteration is of mid-Tertiary age.

The large amount of pyrite in the Shultz Spring zone also suggests that it does not correlate with the Mammoth vein set. Correlation and reconstruction as in figure 7 would put a sulfide zone atop a vein that is sulfidic at depth but oxidic above.

Separation of this magnitude on the San Manuel fault system has implications for the geometry of the upper and lower members of the Cloudburst Formation. Separation of their contact is well over 3,000 m (10,000 ft), a paradox that can be resolved only if the upper and lower members interfinger in the manner shown in figure 18.

RELATION OF CLOUDBURST FAULT TO MID-TERTIARY MINERALIZATION

Spatial and Temporal Relations

The Cloudburst fault is a mid-Tertiary detachment surface, dipping gently east, north of the Turtle fault. It separates underlying Precambrian crystalline rocks from the overlying Cloudburst Formation, which apparently accumulated and was tilted synchronously with fault movement. The proximity and seemingly regular attitude of the Cloudburst detachment surface (fig. 4) suggests that it intersects the part of the Collins vein segment north of the Turtle fault at shallow depth (about 2,900 to 3,000 ft or about 900 m in elevation). All of the Mammoth vein set formed within about 600 m (2,000 ft) of the detachment surface.

The Cloudburst detachment fault is not recorded from underground workings in the Collins vein segment south of the Turtle fault, extending down to about 2,250 ft (685 m) elevation, and does not cut the contiguous San Manuel orebody down to an elevation of about sea level. Neither does the detachment cut the Kalamazoo orebody, which includes a structurally higher interval of even greater thickness. We consider it unlikely that the Cloudburst fault extends south of the Turtle fault, because the structural level of the Cloudburst fault north of the Turtle fault falls in the middle of almost two kilometers of crust where the Cloudburst fault is absent south of the Turtle. More likely, the Turtle fault is a side ramp of the Cloudburst fault; this is consistent with the timing of movement on both faults, which is synchronous with accumulation of Cloudburst Formation and rhyolite intrusion. If so, the strike of the Turtle fault is the direction of movement on the Cloudburst fault, about S. 70° W. (Dickinson, 1991).

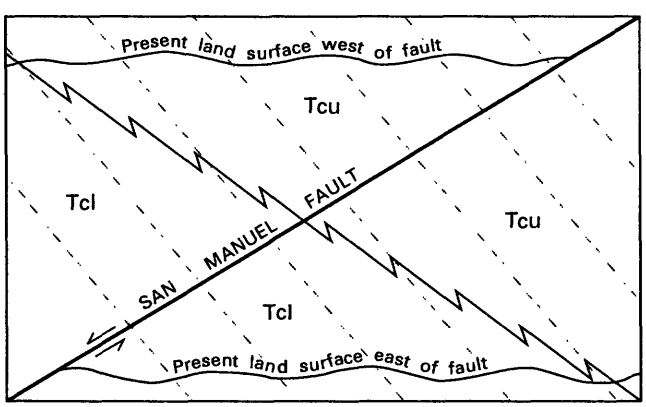

Figure 18. Schematic diagram of relations of the upper (Tcu) and lower (Tcl) members of the Cloudburst Formation necessitated by the calculations of displacement on the San Manuel fault. Zig-zag line indicates facies boundary. Dashed lines represent bedding in the Cloudburst Formation.

The area south of the Turtle fault shows evidence of having been tilted to the east only once. In contrast, the area north of the Turtle fault has been tilted twice, first by the Cloudburst detachment and subsequently by movement of the San Manuel fault system. (Later tilting coeval with Quiburis Formation would affect both sides of the Turtle fault.) The Cloudburst Formation resting unconformably on the Oracle Granite south of the Turtle fault (on both plates of the San Manuel fault system but best exposed on the upper plate) dips about 30°. This absence of two tilting episodes is consistent with either the side-ramp hypothesis or with up-to-the-south offset of the detachment on the Turtle fault, but it is inconsistent with the presence of the Cloudburst detachment at depth south of the Turtle fault and is inconsistent with part of the tilting history advanced by Lowell (1968, his fig. 2). If the Laramide San Manuel porphyry is tilted about 70° as Lowell said, about 40° of this tilting predates the Cloudburst Formation.

Emplacement of the Mammoth vein set closely followed Cloudburst detachment faulting, accumulation of the Cloudburst Formation volcanic rocks and conglomerate, and rhyolite emplacement. That is, the vein set cuts the Turtle fault, the Cloudburst Formation, and rhyolite bodies; however, its silica apparently came from cooling rhyolite, and the vein-associated alteration aureole was a response to heat and fluids from cooling rhyolite and detachment faulting. Mineralization was complete by initial deposition of the San Manuel Formation at 22 Ma.

The close relation of the Mammoth vein set and the Cloudburst detachment fault has no exact counterpart in the Shultz Spring altered area, which is far from the nearest surface exposure of the Cloudburst detachment and structurally is at least 1,050 m (3,450 ft) above it. The Shultz Spring zone is only 185 to 425 m (600 to 1,400 ft) above one strand of the San Manuel fault system but apparently predates that system, based on the absence of alteration of the San Manuel Formation and on the presence of probably correlative alteration in the lower plate of the San Manuel fault system. Alteration in the Shultz Spring area apparently post-dates 22.5 Ma, as Weibel's (1981) potassium feldspar date on tuff probably mixes older primary and younger alteration feldspar, but it predates 22 Ma, the age of basal San Manuel Formation nearby. Thus the age of alteration is tightly constrained in this area.

Probable Genetic Relation

The close spatial and temporal relation of the Cloudburst detachment fault with the Mammoth vein set implies that detachment faulting must have had an effect on mineralization. On the other hand, the timing and geometry of mineralization is not that of detachment mineralization in the strict sense, as described by Spencer and Welty (1986) and Roddy and others (1988). In such deposits, mineralization forms along detachment surfaces and related steep normal faults by circulation of hot fluids during and immediately following fault movement, in response to tectonic denudation. Thus for the Mammoth vein set the exact form of the relation between detachment and mineralization is unclear.

The Mammoth vein set corresponds to the detachment model (Spencer and Welty, 1986; Roddy and others, 1988; Long, 1992) in the following respects:

1. Dominance of oxide-facies over sulfide-facies mineralization.
2. Localization of mineralization near flexures of the detachment surface--in this case under the intersection of the Turtle side-ramp fault and the main Cloudburst detachment fault, based on the geometry of mineral zonation.
3. Early potassium feldspar and sulfide mineralization--in this case early adularia, and slightly later sphalerite, galena, and chalcopyrite.
4. Late oxide-dominated mineralization--in this case wulfenite, vanadinite, manganese oxides, barite, chrysocolla, and malachite. Perhaps cerussite and smithsonite have this origin also.
5. Peripheral barite-manganese oxide-fluorite assemblages.
6. Characteristic amethyst and specularite gangue.
7. Widespread epidote-chlorite alteration--in this case most conspicuous in Tertiary rocks atop the detachment.
8. The elemental assemblage Au-Ag-Ba-Pb-Zn-Cu, commonly without As, Sb, Hg, or Tl.

Some dissimilarities of the Mammoth vein set with the detachment model are these:

9. Mineralization not along the detachment fault but on a cross-cutting structure.
10. Presence of molybdenite and vanadinite. However, the Mammoth vein set is larger and better studied than most deposits that define the model.
11. Association with cooling rhyolite (but see Welty and Spencer, 1986).

Two possible solutions to the problem of the relation between detachment and mineralization are: (1) Rhyolite drove mineralization, but precipitation was in a chemical and physical environment conditioned by immediately previous detachment, and (2) two fluids were necessary for ore formation; one was supplied by rhyolite and the other was transported along the detachment fault. These possibilities could be tested with fluid-inclusion and isotopic studies.

The Shultz Spring altered area may be detachment related, but the evidence is weak. The structural distance above the Cloudburst detachment fault is great, and alteration apparently predates the spatially closer San Manuel fault system. The abundance of pyrite in the Shultz Spring area is apparently unusual for detachment-related mineral systems, as is the bismuth anomaly. Favoring a relation to detachment faulting are the specularite-adularia alteration and the Ba-Mn-Cu-Zn-Au elemental association.

IMPLICATIONS FOR MINERALIZATION

The Mammoth vein set shows intricate spatial and temporal relations both to rhyolite intrusions and to detachment along the nearby Cloudburst-Turtle fault system. Zoning within the vein suggests that the central part of the mineralized system lies under the intersection of the Cloudburst detachment and its Turtle side ramp. Further exploration in this area is warranted, as is examination of the Cloudburst-Turtle fault system itself.

The newly described Shultz Spring alteration is coeval with the Mammoth vein set but is apparently not closely related. Based on reconaissance geochemical sampling, it appears to be weakly mineralized at the surface, but zoning relations suggest pervasive replacement by pyrite at depth.

Some conclusions of this work have implications for the older San Manuel and Kalamazoo deposits. A "backstripping" procedure of progressively removing faults and correlative tilting shows that steep tilting of mid-Tertiary rocks was confined to the domain north of the Turtle fault. South of it, mid-Tertiary tilting is only about 25° to 30°. Thus unless some tilting preceded mid-Tertiary extension, the Laramide San Manuel porphyry was tilted far less than Lowell (1968) believed. This is worthy of further investigation, especially as the San Manuel and Kalamazoo deposits gave rise to models of porphyry zonation.

ACKNOWLEDGMENTS

Lively discussion with W.R. Dickinson in the field and during compilation contributed greatly to many concepts presented here. Table 1 was contributed by Keith Long. Reviewers Robert Kamilli and Keith Long considerably improved the manuscript. Jon Spencer suggested the two-fluid detachment-mineralization concept. Martin Rex of Magma Copper Company facilitated access to workings on the Mammoth vein set. The Shultz Spring altered zone was discussed with Robert Hockett. Discussion with Tim Hait initiated the concept of figure 18.

REFERENCES CITED

Creasey, S.C., 1950, Geology of the St. Anthony (Mammoth) area, Pinal County, Arizona, *in* Arizona zinc and lead

deposits, part 1, chapter 6: Arizona Bureau of Mines Bulletin 156, p. 63-84.

———1965, Geology of the San Manuel area, Pinal County, Arizona: U.S. Geological Survey Professional Paper 471, 64 p.

Dickinson, W.R., 1987, General geologic map of Catalina core complex and San Pedro trough: Arizona Geological Survey Miscellaneous Map MM-87-A (1:62,500).

———1991, Tectonic setting of faulted Tertiary strata associated with the Catalina core complex in southern Arizona: Geological Society of America Special Paper 264, 106 p.

Dickinson, W.R. and Shafiqullah, M., 1989, K-Ar and F-T ages for syntectonic mid-Tertiary volcano-sedimentary sequences associated with the Catalina core complex and San Pedro trough in southern Arizona: Isochron/West, no. 52, p. 15-27.

Goddard, E.N., Parker, D.T., De Ford, R.K., Rove, O.N., Singewald, J.T., Jr., and Overbeck, R.M., 1984, Rock-color chart: Geological Society of America, Boulder, Colorado.

Heindl, L.A., 1963, Cenozoic geology in the Mammoth area, Pinal County, Arizona: U.S. Geological Survey Bulletin 1141-E, 40 p.

Keith, S.B., Gest, D.E., DeWitt, E., Toll, N.W., and Everson, B.A., 1983, Metallic mineral districts and production in Arizona: Arizona Bureau of Geology and Mineral Technology, Bulletin 194, p. 34-35.

Long, K.R., 1992, Preliminary descriptive deposit model for detachment fault-related mineralization *in* Bliss, J.D., ed., Developments in mineral deposit modelling: U.S. Geological Survey Bulletin 2004, p. 52-56.

Lowell, J.D., 1968, Geology of the Kalamazoo orebody, San Manuel district, Arizona: Economic Geology, v. 63, p. 645-654.

Lowell, J.D. and Guilbert, J.M., 1970, Lateral and vertical alteration-mineralization zoning in porphyry ore deposits: Economic Geology, v. 65, p. 373-408.

Motooka, J.M., and Grimes, D.J., 1976, Analytical precision of one-sixth order semiquantitative spectrographic analysis: U.S. Geological Survey Circular 738, 25 p.

Pelletier, J.D., and Creasey, S.C., 1965, Ore deposits, *in* Geology of the San Manuel area, Pinal County, Arizona: U.S. Geological Survey Professional Paper 471, p. 29-59.

Peterson, N.P., 1938, Geology and ore deposits of the Mammoth mining camp area, Pinal County, Arizona: Arizona Bureau of Mines Bulletin 144, 63 p.

Roddy, M.S., Reynolds, S.J., Smith, B.M. and Ruiz, J., 1988, K-metasomatism and detachment-related mineralization, Harcuvar Mountains, Arizona: Geological Society of America Bulletin, v. 100, p. 1627-1639.

Schwartz, G.M., 1953, Geology of the San Manuel copper deposit, Arizona: U.S. Geological Survey Professional Paper 256, 63 p.

Spencer, J.E., and Welty, J.W., 1986, Possible controls of base- and precious-metal mineralization associated with Tertiary detachment faults in the lower Colorado River trough, Arizona and California: Geology, v. 14, p. 195-198.

Steele, H.J., and Rubly, G.R., 1947, San Manuel prospect: American Institute of Mining and Metallurgical Engineers, Technical Publication 2255, 12 p.

Thomas, L.A., 1966, Geology of the San Manuel ore body, *in* Titley, S.R. and Hicks, C.L., eds. Geology of the porphyry copper deposits, southwestern North America: Tucson, University of Arizona Press, p. 133-142.

Weibel, W.L., 1981, Depositional history and geology of the Cloudburst Formation near Mammoth, Arizona: Tucson, University of Arizona, M.S. thesis, 81 p.

Welty, J.W., and Spencer, J.E., 1986, Two types of mineralization related to Tertiary detachment faults in the southwestern United States: Geological Society of America Abstracts with Programs, v. 18, no. 6, p. 785.